# Developing new 4-PIOL and 4-PHP analogues for photo-inactivation of γ-aminobutyric acid type A receptors

*Martin Mortensen[§,ϕ], Jacob Krall[†,ϕ], Kenneth T. Kongstad[†], Benjamin M. Brygger[†], Ombretta Lenzi[†], Pierre Francotte[†,‡], Troels E. Sørensen[†], Birgitte Nielsen[†], Anders A. Jensen[†], Trevor G. Smart[§,*], Bente Frølund[†,*]*

[§] Department of Neuroscience, Physiology & Pharmacology, University College London, Gower Street, London WC1E 6BT, United Kingdom. [†] Department of Drug Design and Pharmacology, Faculty of Health and Medical Sciences, University of Copenhagen, Universitetsparken 2, DK-2100 Copenhagen. [‡] Department of Medicinal Chemistry, Center for Interdisciplinary Research on Medicines (CIRM), University of Liege, Avenue de l'Hôpital, 1, B36, B-4000 Liège, Belgium

**Abstract**

The critical roles played by $GABA_A$ receptors as inhibitory regulators of excitation in the central nervous system has been known for many years. Aberrant $GABA_A$ receptor function and trafficking deficits have also been associated with several diseases including anxiety, depression, epilepsy, and insomnia. As a consequence, important drug groups such the benzodiazepines, barbiturates, and many general anesthetics, have become established as modulators of $GABA_A$ receptor activity. Nevertheless, there is much we do not understand about the roles and mechanisms of $GABA_A$ receptors at neural network and systems levels. It is therefore crucial to develop novel technologies and especially chemical entities that can interrogate $GABA_A$ receptor function in the nervous system. Here, we describe the chemistry and characterization of a novel set of 4-PIOL and 4-PHP analogues synthesized with the aim of developing a toolkit of drugs that can photo-inactivate $GABA_A$ receptors. Most of these new analogues show higher affinities/potencies compared to the respective lead compounds. This is indicative of cavernous areas being present near their binding sites that can be potentially associated with novel receptor interactions. The 4-PHP azide-analogue, **2d**, possesses particularly impressive nanomolar affinity/potency, and is an effective UV-inducible photo-inhibitor of $GABA_A$ receptors with considerable potential for photo-control of $GABA_A$ receptor function *in situ*.

**Keywords**

$GABA_A$ receptors, 4-PIOL, 4-PHP, small ligand organic chemistry, photo-inhibition, single particle tracking, quantum dots.

**Introduction**

Synaptic inhibition in the brain is largely controlled by γ–aminobutyric acid (GABA) where rapid inhibition is mediated by the $GABA_A$ receptors ($GABA_ARs$). This receptor family is abundantly expressed throughout the central nervous system, where they control and modulate a plethora of important physiological processes[1]. Evidence indicates that regulating the numbers of cell surface postsynaptic $GABA_ARs$ represents one of the most powerful mechanisms underlying functional plasticity of GABAergic synapses[2]. Our understanding of $GABA_AR$ cellular distribution and cell surface trafficking profiles is still emerging, but it is clear that dysfunction to underlying mechanisms affecting receptor expression feature in the pathogenesis of a wide range of neurological diseases, especially epilepsy[3-4].

Many approaches for studying receptor trafficking have been used such as expressing tagged recombinant receptors[5-8] or employing antibody-based labelling procedures of native receptors[9-10]. Although valuable, these techniques can be limited by their relative inability to discriminate between functional and non-functional receptors, and between synaptic and extrasynaptic locations, in addition to recombinant receptor expression potentially affecting native receptor subunit composition and function. By contrast, a more direct approach for studying native $GABA_AR$ trafficking is to irreversibly block the orthosteric binding site using a selective high-affinity $GABA_AR$ photoaffinity ligand. Combining this photoaffinity approach with an associated fluorophore would markedly enhance our ability to examine the localization and trafficking of $GABA_ARs$ with higher time and spatial resolution.

Previously, we reported a series of photochemical probes based on the competitive $GABA_AR$ antagonist gabazine. In a range of compounds, we integrated the photo-reactive groups aryl azide, diazirine or benzophenone into the gabazine structure, and demonstrated that the most efficient UV-

induced irreversible block of the GABA binding site (and receptor) was observed with an extended benzophenone analogue called GZ-B1[11].

Here, we report on the design and synthesis of a novel series of photochemical probes engineered for irreversible inactivation and imaging of *native* $GABA_ARs$. The 'modular-design' of these molecules is based on the very weak (low efficacy) partial agonists 5-(4-piperidyl)-3-hydroxyisoxazole (4-PIOL)[12-13] and 4-(4-piperidyl)-1-hydroxypyrazole (4-PHP)[14]. Together these novel compounds constitute a class of highly potent and selective orthosteric $GABA_AR$ ligands. Their potential for cross-linking and visualization of cell surface $GABA_ARs$ was also evaluated.

## Results and Discussion

### Design and synthesis of photoactivated $GABA_AR$ ligands

Photoaffinity labelling is a powerful tool to covalently capture the protein target of small highly specific molecules[15]. However, the design of photoprobes is often challenging due to the difficulty of maintaining the potency, efficacy and specificity of the parent lead compounds while imparting the probes with photo-cross-linking and target visualization capabilities.

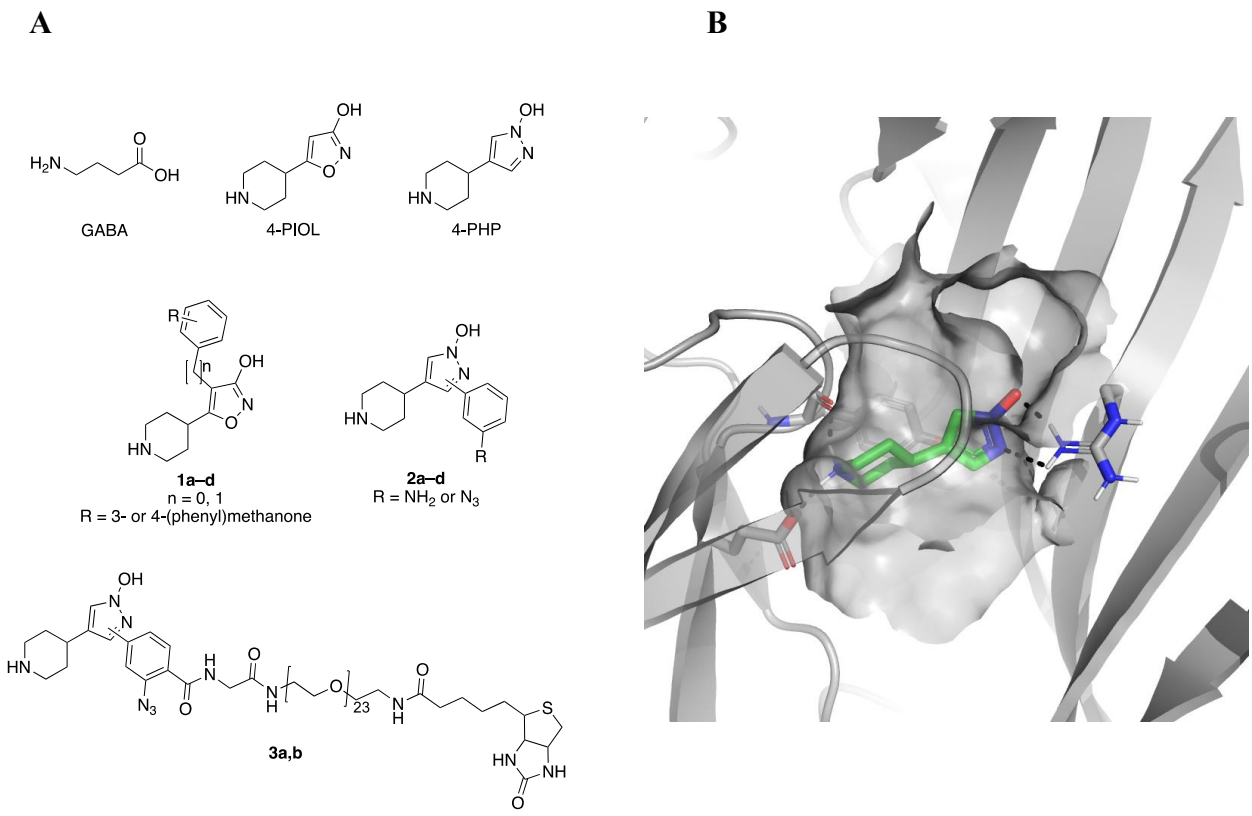


***Figure 1.*** *(A) Structures of GABA, 4-PIOL, 4-PHP, and derivative target structures* ***1a–d***, ***2a–d***, *and* ***3a,b***. *(B) 4-PHP (green carbon atoms) docked into the α1β3γ2 GABA$_A$R homology model (gray carbon atoms) based on the α1β3γ2L cryo-EM structure*[18]*. The surface of the orthosteric binding site and adjacent cavities are displayed in gray. H-bonds are depicted by dashed lines.*

Based on comprehensive structure-activity relationship studies using the core scaffolds of 4-PIOL and 4-PHP (Fig. 1A), we have previously reported on detailed and reliable structural models of the orthosteric $GABA_AR$ binding site[16-17], now facilitated by the latest $GABA_AR$ cryo-EM structures[18-21]. Combining all these structures and models, we have identified several cavities in the GABA (orthosteric) binding site, in close vicinity to the core scaffolds of 4-PIOL and 4-PHP, which are able to accommodate considerable steric bulk (Fig. 1B). Furthermore, several 'ligand-access points' connecting the GABA binding site (under loop C of the β subunit) to the extracellular environment have been identified in $GABA_ARs$.[11] These cavities and 'access points' have also been verified by docking studies using the GABA binding site of homology models based on the recent cryo-EM structures of the human α1β3γ2 heteropentameric $GABA_AR$ in nanodisc bilayers[18-19]. By exploring these binding site cavities with different ligands, we have previously discovered highly potent competitive $GABA_AR$ antagonists, exemplified by 3-phenyl ($K_i$ 0.27 μM, $IC_{50}$ 1.9 μM) and 5-phenyl ($K_i$ 0.022 μM, $IC_{50}$ 0.15 μM) substituted 4-PHP analogues (Table 1)[14, 17, 22]. Interestingly, 3,3-diphenylpropyl-4-PIOL, and the corresponding thio-4-PIOL analogue, displayed a preference for inhibiting tonic compared to phasic $GABA_AR$-mediated currents[23-24]. Therefore, 4-PIOL and 4-PHP constitute useful scaffolds for introducing photoactivatable groups/moieties into the GABA binding site.

Our initial aim was to identify the optimal photoactivatable moiety, and its position within the target scaffold, for photo-cross-linking to the $GABA_AR$ protein. As in our previous study[11], we chose to explore the effects of sequentially incorporating benzophenone or aryl azide as photoactivatable groups into our lead structures of 4-PIOL and 4-PHP. Despite the known photochemistry and chemical reactivities of these groups, which ones are eventually adopted for

inclusion is not straightforward. In some cases, a phenylazide-based photoaffinity probe is preferred, while in other studies benzophenone-based probes are advantageous[25-28]. Based on criteria of stability and synthetic feasibility, the benzophenone and phenylazide moieties were prioritised for incorporation into the 4-position of 4-PIOL (Fig. 1, Scheme 1; **1a**–**d**) and 3- or 5-position of 4-PHP (Fig.1, Scheme 2; **2c**,**d**), respectively.

The benzophenone derivatives of 4-PIOL and the phenyl-azide derivatives of 4-PHP were synthesized as described in Schemes 1 and 2, respectively.

The benzophenone derivatives of 4-PIOL (**1a**–**d**) were synthesized from compound **4**, which was synthesized as described in the literature[29-30], following two distinct strategies (Scheme 1). For the benzophenone derivatives, with the benzophenone directly attached to the 4-isoxazole ring (compounds **1a**,**b**), a Suzuki-Miyaura cross coupling was applied between compound **4** and commercially available (4-benzoylphenyl)boronic acid and phenyl(3-(4,4,5,5-tetramethyl-1,3,2-dioxaborolan-2-yl)phenyl)methanone, following a modified procedure[31]. Acidic deprotection of the intermediates (**5a**,**b**) afforded compounds **1a**,**b**.

The 3- and 4-methylene-benzophenone derivatives of 4-PIOL (**1c**,**d)** were synthesized by a Grignard reaction between compound **4** and 3- or 4-benzoylbenzaldehyde, following a modified procedure[29-30]. 3- and 4-benzoylbenzaldehyde were synthesized from commercially available 3- and 4-benzoylbenzyl bromide, respectively, as previously described in the literature by Miziak et al. (2007)[32] and Suhana and Srinivasan (2003)[33], respectively. Reduction of the formed hydroxyl group (intermediate not shown) using triethylsilane and trifluoroacetic acid followed by acid deprotection of **6c**,**d** afforded compounds **1c**,**d**.

**Scheme 1** [a]

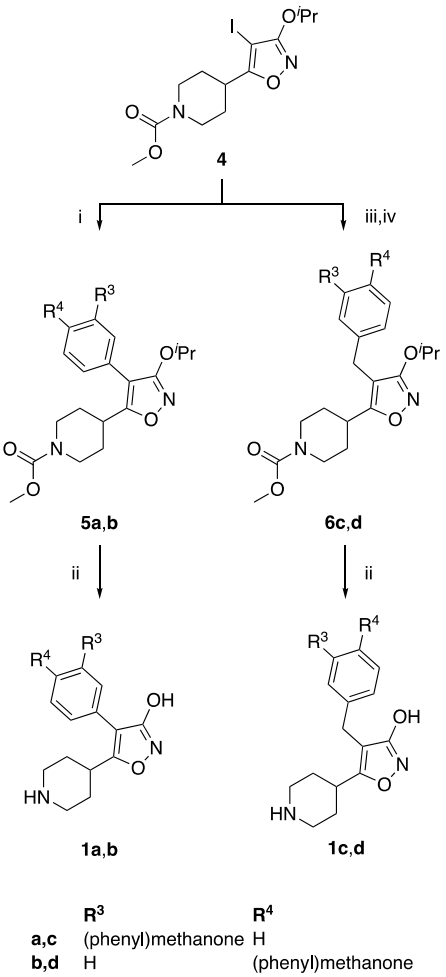


| | R$^3$ | R$^4$ |
|---|---|---|
| **a,c** | (phenyl)methanone | H |
| **b,d** | H | (phenyl)methanone |

[a] *Reagents and conditions: (i) (4-benzoylphenyl)boronic acid or phenyl(3-(4,4,5,5-tetramethyl-1,3,2-dioxaborolan-2-yl)phenyl)methanone, $Pd(PPh_3)_2Cl_2$, $K_2CO_3$, $H_2O$/DMF, 70 °C, (ii) 33% HBr in AcOH, 65 °C, (iii) a)* **4**, $^i$*PrMgCl, THF, –30 °C to 0 °C, b) 3- or 4-benzoylbenzaldehyde, THF, 0 °C to rt., (iv) $Et_3SiH$, TFA, $CH_2Cl_2$, 50 °C.*

The 3- and 5-substituted 4-PHP analogous **2a**–**d** were synthesized as described in Scheme 2 by starting from **10a**,**b**, which were obtained following procedures described previously[14].

The 3-iodinated intermediate **10f**, was synthesized from compound **10a** by first regio-selective iodination in the 3-position using iodine monochloride (**10c**)[14] followed by selective deprotection of the *N*-ethyl-carbamate under basic conditions. The resulting free amine was then re-protected using Boc anhydride and triethylamine to afford compound **10f**. In contrast, the 5-iodinated intermediates **10e** and **10g** were synthesized from compounds **10a** and **10b** using first an ortho-directed metalation with LDA at –78 °C followed by quenching with iodine to afford compound **10d** and **10e**[14]. Compound **10d** was then converted into compound **10g** following an identical approach as described for the conversion of compound **10c** to **10f**.

Suzuki-Miyaura cross-couplings of compounds **10c**–**f** with 3-aminophenylboronic acid afforded compounds **11a**–**d**, where compounds **11a**,**b** were transformed into target compounds **2a**,**b** under acidic conditions. To incorporate the aromatic azide into the target compounds **2c**,**d**, two approaches were used. Compound **11c** was subjected to catalytic hydrogenation using palladium on carbon, thereby resulting in the deprotected hydroxypyrazole **12**, prior to formation of the aromatic azide in compound **13a** using trimethylsilyl azide and *tert*-butyl nitrite. For **11d**, the aniline was converted directly into the aromatic azide, compound **13b**, in analogy to compound **13a**. Compounds **13a**,**b** were then deprotected under acidic conditions to afford compounds **2c**,**d**. Neither of the methods used for synthesizing the comparable aromatic azides **13a** and **13b**, was superior.

**Scheme 2** [a]

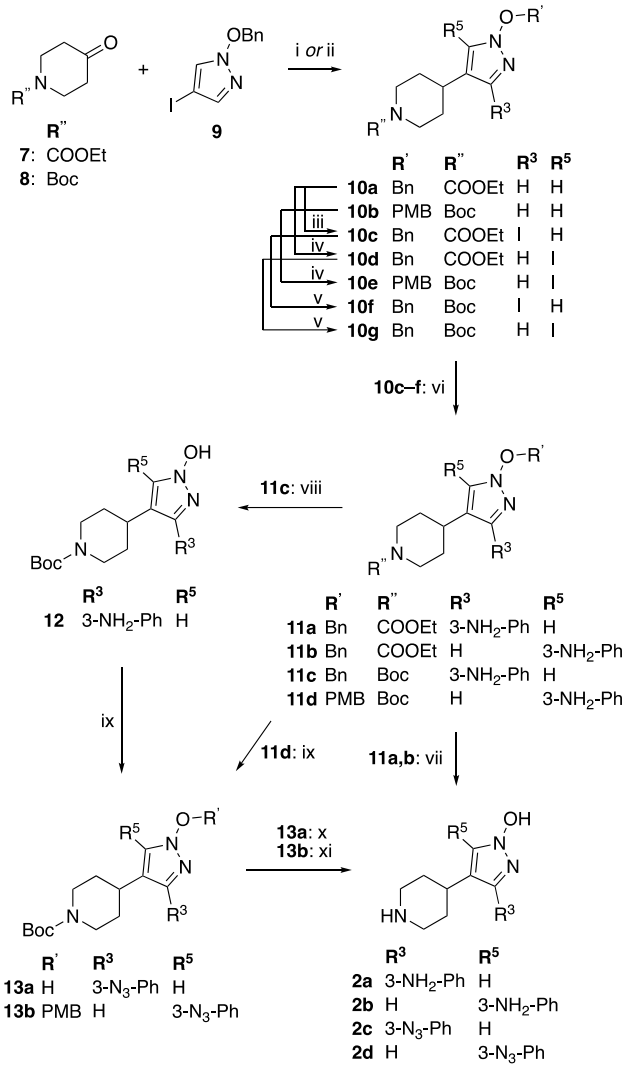


[a] *Reagents and conditions: (i) a) $^{i}$PrMgCl, THF, 0 °C, b) **7**, THF, 0 °C to rt., c) $Et_3SiH$, TFA, $CH_2Cl_2$, 65 °C (ii) a) $^{i}$PrMgCl, THF, 0 °C, b) **8**, THF, 0 °C to rt., c) $H_2$, 10% Pd/C, EtOH, rt., d) PMB-Cl, $K_2CO_3$, acetone, rt., (iii) ICl, AcOH/$H_2O$, 85 °C, (iv) a) **10a** or **10b**, LDA, THF, –78 °C, b) $I_2$, THF, –78 °C to rt., (v) a) KOH, MeOH/$H_2O$, reflux, b) $Boc_2O$, $Et_3N$, $CH_2Cl_2$, (vi) 3-aminophenylboronic acid, $K_2CO_3$, $Pd(PPh_3)_2Cl_2$ or $Pd(PPh_3)_4$, DMF/$H_2O$, 90 °C, (vii) aq. HCl, reflux, (viii) $H_2$, 10% Pd/C, MeOH, rt., (ix) TMS-$N_3$, $^{t}$BuNO$_2$, MeCN, (x) TFA, $CH_2Cl_2$, rt., (xi) HCl, $Et_2O$/EtOH, –78 °C.*

**Pharmacological characterization of the photoactive 4-PIOL $GABA_AR$ ligands.**

The synthesized 4-PIOL analogues (**1a**–**d**) were evaluated for their apparent binding affinities using a [$^3$H]muscimol binding assay with a rat brain cell membrane preparation (Table 1). Using an electrophysiological assay, all the analogues acted as antagonists at recombinant murine α1β2/3γ2 $GABA_ARs$ expressed in HEK293 cells (Figure 2). Therefore, their relative potencies were evaluated by construction of ligand-inhibition curves (Figure 2A) to obtain $IC_{50}$ values for each analogue (Figure 2B; Table 1). In general, the functional data are in good agreement with the binding affinity data (Supplementary Fig. S1).

***Table 1.*** *Pharmacological data for 4-PIOL, the 4-PIOL analogues* ***1a-d****, 4-PHP and the 4-PHP analogues 3- and 5-Ph-4-PHP,* ***2a-d*** *and* ***3a,b****. $GABA_AR$ binding affinities at rat cortical cell membranes and functional properties at α1β2/3γ2 $GABA_AR$ transiently expressed in HEK293 (whole cell patch clamp) or tsA201 cells (FMP assay).*

| | [$^3$H]muscimol binding $K_i$ (μM) [p$K_i$ ± SEM] | $IC_{50}$ (μM) [p$IC_{50}$ ± SEM] |
|---|---|---|
| **4-PIOL** | 9.1[e] | > 500 [< 3.30][e] |
| **1a** | 0.018 [7.75 ± 0.01] | 0.008 [8.09 ± 0.12][a] |
| **1b** | 0.16 [6.80 ± 0.05] | 0.10 [6.99 ± 0.11][a] |
| **1c** | 0.47 [6.33 ± 0.01] | 0.18 [6.75 ± 0.11][a] |
| **1d** | 0.60 [6.22 ± 0.06] | 0.24 [6.63 ± 0.14][a] |
| **4-PHP** | 10 [4.99 ± 0.02][f] | > 500 [< 3.30][f] |
| **3-Ph-4-PHP** | 0.27 [6.57 ± 0.01][f] | 1.9 [5.73 ± 0.06][c, f] |
| **5-Ph-4-PHP** | 0.022 [7.65 ± 0.02][f] | 0.15 [6.81 ± 0.04][c, f] |
| **2a** | 0.27 [6.57 ± 0.06] | 1.8 [5.75 ± 0.11][d] |
| **2b** | 0.017 [7.79 ± 0.07] | 0.065 [7.19 ± 0.05][d] |
| **2c** | 0.22 [6.66 ± 0.04] | 0.21 [6.68 ± 0.07][b] |
| **2d** | 0.023 [7.66 ± 0.08] | 0.028 [7.55 ± 0.09][b] |
| **3a** | 32 [4.54 ±0.10] | 5.3 [5.28 ± 0.09][b] |
| **3b** | 1.1 [6.00 ± 0.11] | 0.73 [6.14 ± 0.12][b] |

*The apparent binding affinity constant, $K_i$, was obtained from binding experiments on rat brain cell membranes, whereas the functional potencies of the antagonist analogues were obtained from concentration-inhibition experiments as $IC_{50}$ values. In functional studies, $GABA_A$Rs were transiently expressed as: [a]α1β2γ2 or [b]α1β3γ2 in HEK293 cells and tested in whole-cell voltage clamp experiments, or as human α1β2γ2 in tsA201 cells and tested in FMP [c]Red or [d]Blue assay. [e]Data from Frølund et al., 2005[29], and [f]Data from Møller et al., 2010[14]. Mean values ($K_i$ and $IC_{50}$) are shown, along with $pK_i$ ± SEM and $pIC_{50}$ ± SEM values, from 4 – 8 experiments.*

The benzophenone-4-PIOL photoaffinity probes, **1a**–**d**, all showed binding affinities in the high to low nanomolar range, most likely because the lipophilic benzophenone affects the desolvation energy, which is not inherent in the lead molecule, 4-PIOL ($K_i$ 9.1 μM, Table 1). The observation that the bulky benzophenone analogues **1a**–**d** bind to the orthosteric $GABA_AR$ binding site with high apparent affinity further supports the presence of cavities capable of accommodating relatively large substituents near the 4-PIOL scaffold.

The highest binding affinity and functional potency was observed for analogue **1a** ($pK_i$: 7.75 ± 0.01; and $pIC_{50}$: 8.09 ± 0.12, respectively; Table 1), where the benzophenone substituent is directly connected to the 4-PIOL scaffold via the 3-phenyl position. This affinity/potency was >10-fold higher than those observed for the longer analogues, **1b** and **1c**, as well as for the same length analogue with benzophenone connected to 4-PIOL via the adjacent 4-phenyl position (Fig. 2A-B; Table 1).

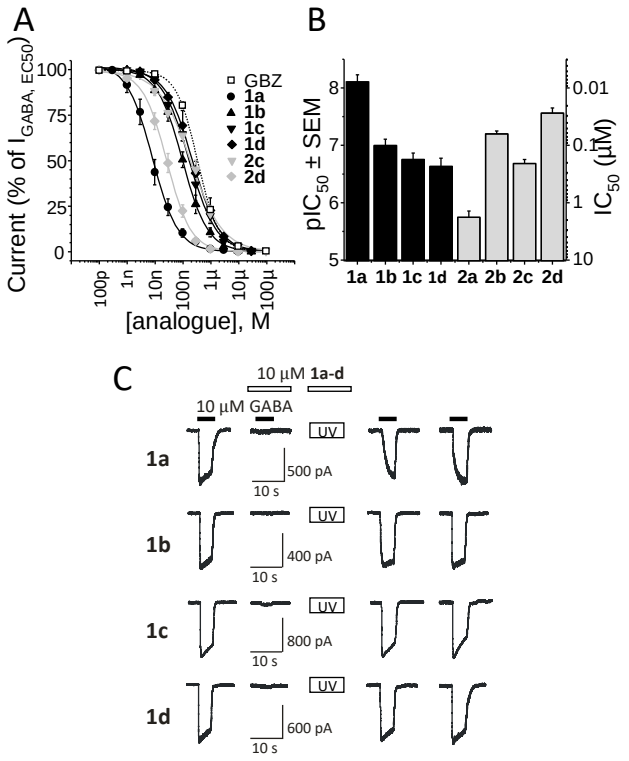


***Figure 2.*** *(A) Ligand concentration inhibition curves for 4-PIOL [**1a-d**] and 4-PHP analogues [**2a-d**] on α1β2γ2 $GABA_A$Rs expressed in HEK293 or tsA201 cells using whole-cell patch clamping or FMP assay (see Table 1 for details); mean ± sem, n = 4-12; (B) Potencies of analogues are shown as $pIC_{50}$ ± SEM [linear y-axis, left] and as mean $IC_{50}$ [Log y-axis, right]; (C) GABA current examples showing that the 4-PIOL analogues all failed to induce UV ($\lambda_{375}$) photo-inhibition (i.e. no depression of the GABA induced currents post-UV treatment).*

The four 4-PIOL analogues, **1a**-**d**, were examined in whole-cell patch clamp experiments for their ability to photo-inactivate α1β2γ2 $GABA_A$Rs expressed in HEK293 cells (Fig. 2C). A concentration of 10 µM GABA, which induces a sub-maximal current with this receptor isoform, was efficiently blocked by co-application with 10 µM of either of the competitive antagonist analogues, **1a**-**d**. The orthosteric binding sites were then fully occupied by 10 µM of **1a**-**d** while

being exposed to UV light for 10 s to induce photo-activation of the analogues, with the intention of covalent bonding to residues within the GABA binding site. After thorough wash-out of non-covalently bound 4-PIOL analogues, 10 μM of GABA was re-applied to the cells. However, none of the four analogues (**1a**-**d**) irreversibly inhibited the GABA-induced currents which were of identical amplitudes to those observed prior to UV treatment (Fig. 2C). This suggested a failure of covalent binding to the GABA site. We next chose to assess if the 4-PHP scaffold would be a better lead molecule in the development of photo-reactive $GABA_AR$ blockers.

**Pharmacological characterization of the photoactive 4-PHP $GABA_AR$ ligands.**

We have previously observed that introducing a phenyl group into either position 3- or 5- of 4-PHP, the 5-phenyl-4-PHP analogue displayed a >10-fold higher affinity, and functional potency as an antagonist at $GABA_ARs$, in comparison with 3-phenyl-4-PHP ($pK_i$: 7.65 ± 0.02 and $pIC_{50}$: 6.81 ± 0.04 versus $pK_i$: 6.57 ± 0.01 and $pIC_{50}$: 5.73 ± 0.06, respectively; Table 1)[9]. This preference for the 5-position corresponded well with the data we obtained when introducing an amino group into the phenyl group of either 3-phenyl-4-PHP or 5-phenyl-4-PHP, **2a** ($pK_i$: 6.57 ± 0.06 and $pIC_{50}$: 5.75 ± 0.11; Table 1) and **2b** ($pK_i$: 7.79 ± 0.07 and $pIC_{50}$: 7.19 ± 0.05; Fig. 2B, Table 1), respectively, where no impact was observed on either ligand affinity for, or potency at, $GABA_ARs$.

After establishing that an amino substituent was tolerated in the 3-position on the phenyl ring, we next replaced the amino group in **2a** and **2b** with a photo-reactive azide group to generate **2c** (analogous to **2a**) and **2d** (analogous to **2b**). With these analogues we observed no change in affinity, but a modest reduction in the inhibitory potency when compared with **2a** and **2b** (**2c**, $pK_i$: 6.66 ± 0.04 and $pIC_{50}$: 6.68 ± 0.07; and **2d**, $pK_i$: 7.66 ± 0.08 and $pIC_{50}$: 7.55 ± 0.09; Fig. 2B, Table

1). As the photo-reactive 5-(3-azidophenyl)-4-PHP, **2d**, displayed significantly higher affinity and potency for α1β2γ2 $GABA_A$Rs than 3-(3-azidophenyl)-4-PHP (**2c**; both $p < 0.0001$), we decided to proceed by testing the photo-inhibition properties of **2d**.

We performed photo-inhibition experiments similar to those with the benzophenone-4-PIOL analogues (**1a-d)**, but now using 5-(3-azidophenyl)-4-PHP (**2d**). Interestingly, a substantive irreversible inhibition (~70%) of 10 μM GABA currents was observed (Figure 3A, B), indicating efficient covalent integration of the UV-activated **2d** analogue into the GABA binding site. The GABA $EC_{50}$ values before and after UV treatment in the absence of a PHP ligand were identical ($pEC_{50}$: 5.39 ± 0.18 [$EC_{50}$: 4.1 μM, n = 5], and $pEC_{50}$: 5.16 ± 0.24 [$EC_{50}$: 6.8 μM, n = 5], respectively; p = 0.48; Figure 3C), which suggested that the function of $GABA_A$Rs in the cell preparation were unaffected by UV exposure. However, in the presence of PHP ligand, the pronounced depression of the maximum GABA current responses was indicative of irreversible antagonist behavior by **2d** at α1β2γ2 $GABA_A$Rs after UV; i.e. a covalent block of ~75% of all GABA binding sites (Figure 3C). Interestingly, this new photo-reactive azide-5-phenyl-4-PHP ligand, **2d**, was more effective than our previous photo-antagonist which was based on gabazine, GZ-B1, which maximally achieved ~50% irreversible inhibition[11]. We attribute the improved photo-inhibition to the higher affinity of **2d** for the GABA binding site compared with that of GZ-B1 (**2d**: 23 nM; versus GZ-B1: 153 nM[11]).

It is possible that further photo-inhibition could have been achieved with multiple rounds of UV exposure with **2d**, but since damage to cell health using such protocols is significant and thus detrimental to the longevity of electrophysiology recordings, we chose not to pursue this.

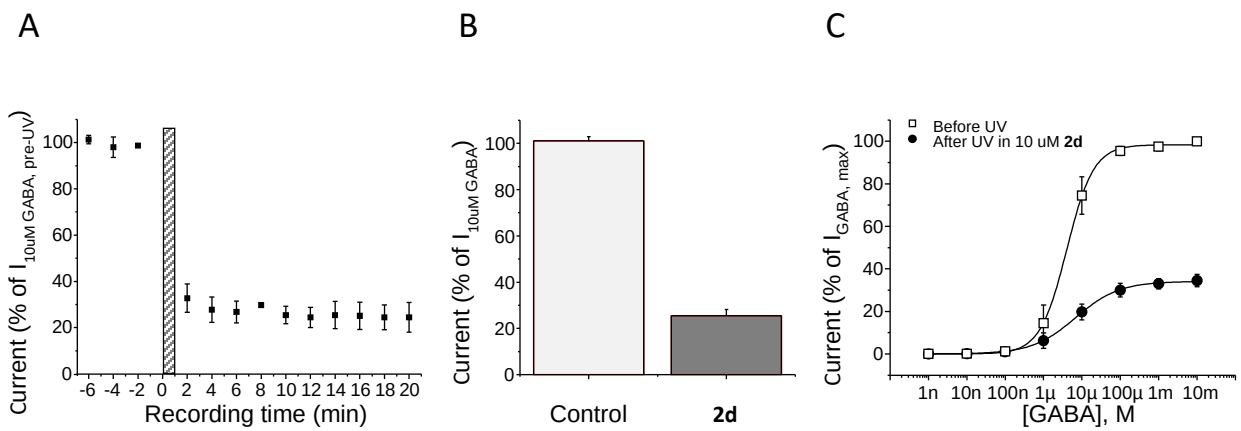


***Figure 3.*** *(A) Efficient photo-inactivation of α1β2γ2 $GABA_A$Rs expressed in HEK293 cells by* ***2d*** *(10 μM); 10s of UV [hatched bar], n = 10; (B) level of photo-inhibition 5 min after UV exposure of Krebs solution [control] or 10 μM* ***2d*** *and washout of non-covalently bound drug; (C) GABA concentration-response curves before and after UV exposure with* ***2d*** *showing irreversible inhibition ('before-UV' Hill curve parameters: Vmax: 98 ± 1.2 %, $EC_{50}$: 4.1 μM, slope: 1.4 ± 0.1, n = 5; 'after-UV' Hill curve parameters: Vmax: 34 ± 2.8 %, $EC_{50}$: 6.8 μM, slope: 1.1 ± 0.1, n = 5). All data are shown as mean ± sem.*

Given the increased inhibitory efficacy we developed a novel biotin-linked **2d**-analogue for receptor trafficking studies. The advantage of adapting a ligand such as **2d** into a trafficking probe, is that we can study native $GABA_A$Rs without the need for prior introduction of epitope tags or mutations to the receptors.

**Design, synthesis and pharmacological characterization of photo-conjugates engineered for photo-cross-linked imaging**

In previous trafficking studies of GABA receptors (both $GABA_A$ and $GABA_B$ receptors) we have relied on the introduction of an α-bungarotoxin binding site mimotope into $GABA_A$R subunits and

coupling α-bungarotoxin to quantum dots (QDs) via biotin-streptavidin ultra-high affinity binding[8]. The bright fluorescence emitted by the QDs could then be tracked in live imaging studies of receptor movements in cell membranes of hippocampal neurons[34].

To assess native $GABA_A$Rs we successfully developed a gabazine analogue GZ-B1-biotin which could be used in trafficking studies[4]. However, despite some success, this ligand did not display sufficiently robust specific binding. We therefore developed another $GABA_A$R photo-probe based on the 4-PHP analogue, **2d**, reasoning that the increased photo-inhibition, and higher binding affinity and potency over GZ-B1 might improve the level of receptor labelling.

The hydrophilic polyethylene glycol (PEG) linker utilized in GZ-B1-biotin was very short (only 2 units long), so we speculated that this could be one reason why specific binding to streptavidin-$QD_{655}$ was compromised. As the $QD_{655}$ molecule (6-12 nm[35]) is of a similar size to the extracellular part of a $GABA_A$R (6-9 nm; measurements made on the cryo-EM structure of human α1β3γ2 $GABA_A$Rs with truncated N-terminus, pdb: 6I53[18]) it is reasonable to assume that more distance between the two globular entities ($GABA_A$R ECD and $QD_{655}$-streptavidin/biotin-**2d)**, would be required to allow unhindered specific binding by the tethered ligand.

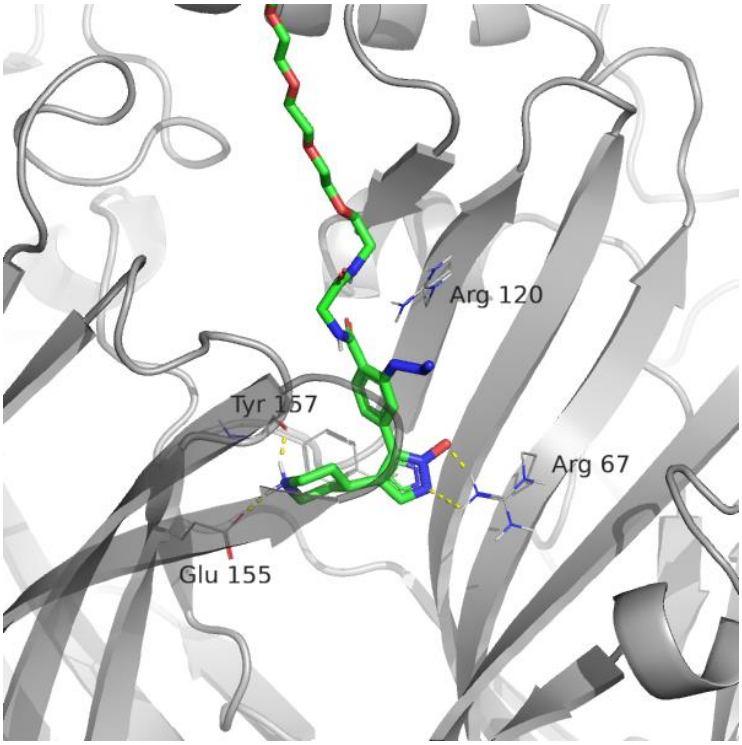


***Figure 4. 3b*** *bound to the human α1β3γ2 GABA$_A$R orthosteric binding site. Receptor carbon atoms are shown in gray,* ***3b*** *carbon atoms in green, hydrogen bonds shown as yellow dashes.*

We estimated the optimal PEG linker length from ligand-receptor docking studies of various target **2d-**photoprobe analogues into the GABA binding site (Figure 4). Allowing for PEG flexibility, for plenty of space for the PEG linked to the PHP-core to exit the binding site, and for the conjugated biotin to gain some distance from the GABA$_A$R and be able to interact with streptavidin unhindered, we deduced a longer 23-unit PEG (PEG$_{23}$) linker was required.

To study the effects of the biotin attachment via a PEG$_{23}$ on the binding affinity to and functionality of the GABA$_A$R, we synthesized analogues based on both **2c** and **2d**, leading to the target analogues, **3a** and **3b**, respectively.

**Scheme 3** [a]

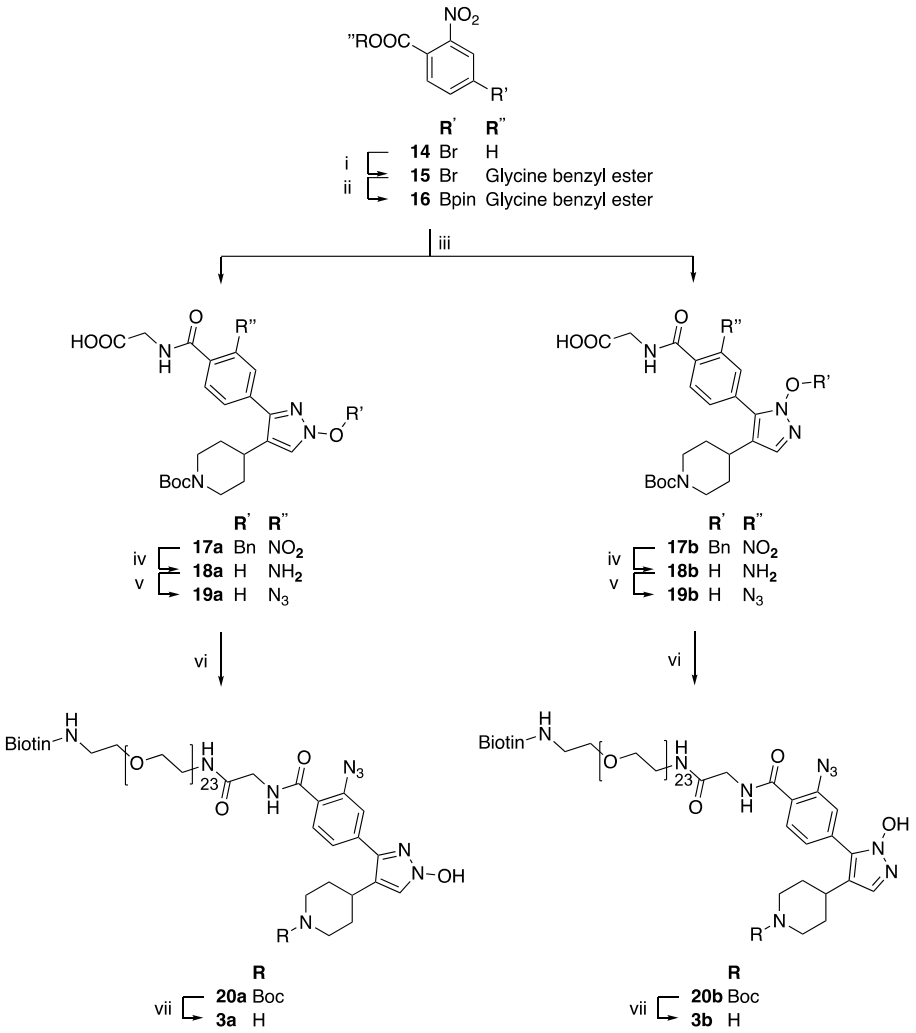


[a] *Reagents and conditions: (i) CDI, Benzyl glycinate, DMF, 0 °C to rt., (ii), $(Bpin)_2$, KOAc, $Pd(dppf)Cl_2 \cdot CH_2Cl_2$, 1,4-Dioxane, 100 °C, (iii) Compound* ***16***, ***10f*** *or* ***10g***, $K_2CO_3$, $Pd(PPh_3)_4$, DMF/$H_2O$ (2:1), 90 °C, (iv) $H_2$, 10% Pd/C, DMF, rt., (v) TMS-$N_3$, $^tBuNO_2$, MeCN/THF, 0 °C to rt., (vi) PyBOP, DiPEA, Biotin-$PEG_{23}$-$NH_2$, DMF, rt., (vii) TFA, $CH_2Cl_2$, 0 °C to rt.*

The synthesis was performed as described in Scheme 3 starting from commercially available 4-bromo-2-nitrobenzoic acid (**14**). Extending the carboxylic acid with a glycine benzyl ester using carbonyldiimidazole formed compound **15**, which was converted into a suitable Suzuki-Myiaura cross coupling reagent using bis(pinacolato)diboron ($Bpin_2$) and $Pd(dppf)Cl_2 \cdot CH_2Cl_2$ in anhydrous

1,4-dioxane at elevated temperatures (MW irradiation). The resulting compound **16** (black tar) was observed unstable towards standard purifications (flash column chromatography and standard normal and reverse phase HPLC, data not shown) and was prepared freshly before each cross-coupling reaction and without purification.

Suzuki-Myiaura cross-coupling between compound **16** and either **10f** or **10g** afforded compounds **17a** and **17b** respectively, where the loss of the benzyl ester of the glycine residue was observed. Compounds **17a**,**b** were subjected to catalytic hydrogenation using palladium on carbon and the resulting anilines (**18a**,**b**) were converted into aromatic azides (**19a**,**b**) using tetramethylsilyl azide and *tert*-butyl nitrite. Incorporation of the Biotin-$PEG_{23}$-$NH_2$ moiety in compound **20a**,**b** was performed by applying peptide chemistry methodologies using PyBOP and DiPEA at room temperature. The resulting **20a**,**b** were then deprotected under acidic conditions (trifluoroacetic acid) to afford compounds **3a**,**b**.

Binding and functional experiments with **3a** and **3b**, re-affirmed that substitution in the 5-position in 4-PHP, **3b** (p$K_i$: 6.03 ± 0.11 and $pIC_{50}$: 6.14 ± 0.12), resulted in more potent ligands compared to substitution in the 3- position, **3a** (p$K_i$: 4.54 ± 0.10 and $pIC_{50}$: 5.28 ± 0.09; Figure 5B and Table 1). However, the $PEG_{23}$-biotin conjugation resulted in a 25-fold loss of affinity/potency when compared with the parent analogues (**2c** and **2d**; Table 1).

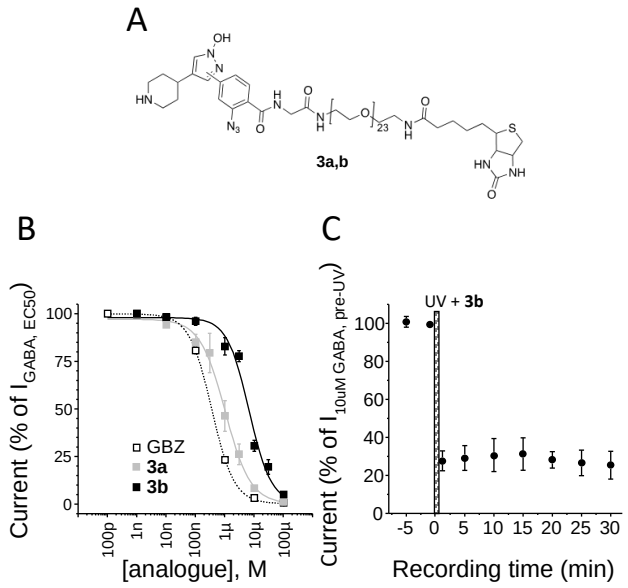


***Figure 5.*** *(A) Generalised chemical structures of **3a** and **3b**, showing biotin linked to the parent analogues [**2d** and **2c**, respectively] via a PEG linker; (B) Ligand concentration inhibition response curves for **3a** and **3b** in relation to gabazine (GBZ, n = 6 -12); (C) irreversible UV photo-inhibition by **3b** (10 µM; n = 7; 10 sec of UV at t = 0 [hatched bar]). Whole-cell patch clamp data in (B and C) was from α1β2γ2 GABA$_A$Rs expressed in HEK293 cells; all data are mean ± sem.*

Photo-inhibition experiments successfully showed that the level of UV-stimulated irreversible block of recombinant α1β3γ2 GABA$_A$Rs was largely unchanged for **3b** (~70%) when compared with **2d** (~70–75%), indicating that the photo-reactive azide group remains functionally available after ligand binding to the orthosteric site.

The final step in our assessment of **3b** was to test its utility at labelling and tracking of GABA$_A$Rs using QD$_{655}$-streptavidin. Unfortunately, after having exhausted several different methods, and a range of concentrations, incubation times, UV exposures, we failed to obtain any useful labelling of receptors (Supplementary Fig. S2; video 1). This was very disappointing as controls of our

methodology with an engineered $GABA_A$ α1 subunit with an N-terminus bungarotoxin site ($\alpha1_{BBS}$) expressed with β2 and γ2 subunits were perfectly fine with clear demonstration of specific binding (Supplementary Fig. S3; video 2).

We deduce that the reason for the lack of specific binding of **3b**-$QD_{655}$ to $GABA_ARs$, probably resides with the long $PEG_{23}$ which may have coiled or become adsorbed to the protein surface potentially obscuring the biotin molecule, thereby hindering binding to streptavidin. However, the observed affinity and potency allude to dynamic regions near the orthosteric binding site and connectors to the extracellular environment, adaptable to substituents of various nature and size.

**Conclusion**

We have synthesized and characterized a series of novel 4-PIOL and 4-PHP photo-probes. All these bulky photo-reactive analogues (**1a-d**, **2c-d**) show higher affinity and potency for the GABA binding site than their lead compounds, indicating considerable spaciousness in the GABA binding site and additional anchoring points between ligand and the $GABA_AR$. The 4-PHP azide-analogue, **2d**, showed remarkable nanomolar affinity, as well as efficient photo-inactivation for the $GABA_AR$ and can serve as a useful research tool of native receptors. Combining this probe with precise UV-delivery could prove to be a powerful technology in the advancement of our understanding of $GABA_AR$ function and effect.

## Methods

### *Chemistry*

Compounds **4**[29-30], **9**[36], **10a**,**c**,**d**[7], 3-benzoylbenzaldehyde[32], and 4-benzoylbenzaldehyde[33] were all synthesized as described in the literature. All reagents and solvents (reagent or chromatography grade) were obtained from commercial suppliers and used without further purification. Air- and/or moisture-sensitive reactions were performed under a nitrogen atmosphere using syringe-septum cap techniques and with the use of flame-dried glassware. Anhydrous solvents were obtained by using a solvent purification system (THF) or by storage over 3 Å molecular sieves. Thin layer chromatography (TLC) was carried out using Merck silica gel 60 $F_{254}$ plates, and compounds were visualized using UV (254 and 366 nm), $KMnO_4$ or Ninhydrin spray reagent. Flash column chromatography (FC) and dry column vacuum chromatography (DCVC) were performed using Merck silica gel (0.040–0.063 mm or 0.015–0.040 mm, respectively). Preparative reversed phase HPLC was performed on an Agilent 1100 system, equipped with two preparative solvent delivery units, a multiple wavelength detector (210 or 254 nm), an autosampler injector (1 mL Loop) and an optional fraction collector, using a preparative Phenomenex Luna C18(3) column (21.2 mm × 250 mm, 5 μm, 100 Å) and Eluent A (acetonitrile/water/HCOOH, 5:95:0.1) and Eluent B (acetonitrile/water/HCOOH, 95: 5:0.1) at a flowrate of 20 mL/min. The column was operated at rt. For HPLC control, data collection, and data handling, ChemStation ver. 3.02 was used. Melting points were recorded on a SRS OptiMelt apparatus in open capillary tubes and are uncorrected. $^{1}H$ and $^{13}C$ NMR data were recorded on a 300 MHz Varian Mercury 300BB spectrometer equipped with a 5 mm $^{1}H$(BB) probe, a 300 MHz Varian Gemini 2000BB spectrometer equipped with a 5 mm $^{31}P$, $^{13}C$($^{1}H$, $^{19}F$) probe, a Bruker Avance 400 MHz spectrometer equipped with a 5 mm PABBO BB($^{1}H$, $^{19}F$) Z-GRD probe, a Bruker Avance 600 MHz spectrometer equipped with a

cryogenically cooled 5 mm CPDCH $^{13}C(^{1}H)$ Z-GRD probe, or a Bruker Avance 600 MHz spectrometer equipped with a cryogenically cooled 1.7 mm CPTCI $^{1}H(^{13}C, ^{15}N)$ Z-GRD probe at 300 K. Data are tabulated in the following order: chemical shift (δ) [multiplicity (b, broad; s, singlet; d, doublet; t, triplet; q, quartet; p, pentet; m, multiplet), coupling constant(s) *J* (Hz), number of protons. The solvent residual peak was used as internal reference.[37] Quantification of salt-free **3a** and **3b** were performed by the standard Bruker method, ERETIC2 in Topspin 3.5, using pulse width optimized 1D $^{1}H$ experiments with long relaxations delay between transients, with cinnamic acid as external standard. Analytical High performance liquid chromatography (anal. HPLC) was performed on a Merck-Hitachi HPLC system consisting of an L-7100 pump, an L-7200 auto sampler, and an L-7400 UV detector (210 or 254 nm), using a Chromolith SpeedROD RP-18 column (4.6 × 50 mm). A linear gradient elution was applied with eluent A ($H_2O$/TFA 100:0.01) containing 0% of solvent B (MeCN/$H_2O$/TFA, 90:10:0.01) rising to 100% of B over 3.5 min with a flow rate of 4.0 mL/min. The purity of the analyzed compounds is ≥95% unless otherwise stated. Data were acquired and processed using the EZChrom Elite Software version 3.1.7 by Hitachi. HPLC-HRMS analyses were performed on a system comprised of an Agilent 1200 HPLC system comprising of a quaternary pump with a built-in degasser, a thermostated column compartment, an autosampler, and a photodiode array detector, coupled with a Bruker microOTOF-QII mass spectrometer equipped with an electrospray ionization (ESI) source and operated via a 1:99 flow splitter. Mass spectra were acquired in positive ionization mode, using drying temperature of 200 °C, a capillary voltage of −4100V, nebulizer pressure of 2.0 bar, and drying gas flow of 7 L/min. A solution of sodium formate clusters was injected in the beginning of each run to enable internal mass calibration. Chromatographic separation was acquired on a Phenomenex Luna C18(2) column (150 mm × 4.6 mm, 3 μm, 100 Å) maintained at 40 °C, using a flow rate of 0.8 mL/min

and a linear gradient of the binary solvent system water-acetonitrile-formic acid (eluent A: 95/5/0.1, and eluent B: 5/95/0.1) rising from 0% to 100% of eluent B over 20 minutes. Data was acquired using Compass HyStar Ver. 3.2 (Bruker Daltonic GmbH, Germany) and processed using Compass DataAnalysis Ver. 4.0 (Bruker Daltonic GmbH, Germany).

**(3-(3-hydroxy-5-(piperidin-4-yl)isoxazol-4-yl)phenyl)(phenyl)methanone (1a).** A solution of **5a** (0.17 g, 0.4 mmol) in 33% HBr in AcOH (4 mL) was stirred at 65 °C for 18 h. Upon cooling to rt., the reaction mixture was evaporated *in vacuo.* Recrystallization from EtOH/$Et_2O$ afforded compound **1a** as white crystals (0.48 g, 37%): mp 209–211 °C. $^1$H NMR (300 MHz, $D_2O$): δ 7.76–7.47 (m, 9H), 3.46–3.42 (m, 2H), 3.25–3.15 (m, 1H), 3.04–2.94 (m, 2H), 2.08–1.96 (m, 4H). $^{13}$C NMR (300 MHz, $D_2O$): δ 200.1, 170.5, 168.7, 137.4, 136.7, 133.9, 130.8, 130.5, 130.0, 129.4, 128.8, 128.2, 112.7, 107.2, 43.6, 32.0, 26.1.

**(4-(3-hydroxy-5-(piperidin-4-yl)isoxazol-4-yl)phenyl)(phenyl)methanone (1b).** A solution of **5b** (0.56 g, 1.2 mmol) in 33% HBr in AcOH (4 mL) was stirred at 65 °C for 18 h. Upon cooling to rt., the reaction mixture was evaporated *in vacuo.* Recrystallization from MeOH/$H_2O$ afforded compound **1b** as white crystals (0.25 g, 60%): mp. 227–221 °C (decomp.). $^1$H NMR (300 MHz, DMSO-$d_6$): δ 11.97 (b s, 1H), 8.63 (b s, 1H,), 7.82–7.55 (m, 9H), 3.39–3.34 (m, 3H), 3.12–2.97 (m, 2H), 2.05–1.91 (m, 4H). $^{13}$C NMR (300 MHz, DMSO-$d_6$): δ 195.9, 171.1, 168.9, 137.7, 136.4, 133.8, 133.5, 130.9, 130.4, 129.4, 129.4, 106.4, 46.8, 32.5, 27.2.

**(3-((3-hydroxy-5-(piperidin-4-yl)isoxazol-4-yl)methyl)phenyl)(phenyl)methanone (1c).** A solution of **6c** (0.25 g, 0.5 mmol) in 33% HBr in AcOH (5 mL) was stirred at 65 °C for 18 h. Upon cooling to rt., the reaction mixture was evaporated *in vacuo.* Recrystallization from EtOH/water afforded compound **1c** as white crystals (0.17 g, 89%): mp 225–227 °C (decomp.). $^1$H NMR (300 MHz, $D_2O$): δ 7.69–7.38 (m, 9H), 3.70 (s, 2H), 3.47–3.38 (m, 2H), 3.19–2.91 (m, 3H), 1.99–1.82

(m, 2H). $^{13}$C NMR (300 MHz, $D_2O$): δ 200.9, 171.1, 170.2, 139.4, 137.3, 137.0, 133.7, 133.4, 130.4, 130.1, 129.2, 128.7, 128.5, 105.0, 43.7, 31.7, 26.0.

**(4-((3-hydroxy-5-(piperidin-4-yl)isoxazol-4-yl)methyl)phenyl)(phenyl)methanone (1d).** A solution of **6d** (0.19 g, 0.4 mmol) in 33% HBr in AcOH (4 mL) was stirred at 65 °C for 18 h. Upon cooling to rt. the reaction mixture was evaporated *in vacuo.* Recrystallization from water afforded compound **1d** as white crystals (0.14 g, 94%): mp 118–120 °C (decomp.). $^1$H NMR (300 MHz, $D_2O$): δ 7.45–7.32 (m, 5H), 7.24 (t, $J$ = 7.0 Hz, 2H), 7.10 (d, $J$ = 6.75 Hz, 2H), 3.60 (s, 2H), 3.42–3.38 (m, 2H), 3.13–2.92 (m, 3H), 2.01–1.78 (m, 4H). $^{13}$C NMR (300 MHz, $D_2O$): δ 197.8, 170.7, 169.8, 144.9, 136.7, 134.8, 133.0, 130.6, 129.9, 128.4, 128.3, 104.2, 43.6, 31.6, 30.8, 26.4, 26.1.

**3-(3-aminophenyl)-4-(piperidin-4-yl)-1*H*-pyrazolol (2a).** Compound **11a** (0.24 g, 0.6 mmol) was dissolved in 35% aq. HCl (10 mL) and refluxed at 130 °C for 2h. The reaction mixture was cooled to rt. and evaporated *in vacuo.* The resulting residue was re-evaporated twice with water (10 mL) and twice with toluene (10 mL). Purification by recrystallization from MeOH/$Et_2O$ brought **2a** (115 mg, 58%) as light brown crystals: mp 212–214 °C. $^1$H NMR (600 MHz, MeOD-$d_4$): δ 7.71–7.69 (m, 1H), 7.64 (t, $J$ = 1.8 Hz, 1H), 7.62 (t, $J$ = 7.9 Hz, 1H), 7.55 (s, 1H), 7.38 (ddd, $J$ = 7.7, 2.0, 0.7 Hz, 1H), 3.46–3.41 (m, 2H), 3.25–3.17 (m, 3H), 2.15–2.10 (m, 2H), 1.85–1.77 (m, 2H). $^{13}$C NMR (150 MHz; MeOD-$d_4$): δ 140.1, 135.5, 131.2, 130.3, 127.9, 122.0, 454.7, 121.6, 120.4, 44.0, 30.1, 29.7. Purity by anal. HPLC (254 nm), > 99%.

**5-(3-Aminophenyl)-4-(piperidin-4-yl)-1*H*-pyrazolol (2b). 11b** (0.24 mg, 0.6 mmol) was dissolved in 35% aq. HCl (100 mL) and refluxed at 130 °C for 1 h. The reaction mixture was cooled to rt. and evaporated *in vacuo.* The resulting residue was re-evaporated with 48% aq. HBr *in vacuo*. Purification by recrystallization from MeOH/$Et_2O$ brought **2b** (0.19 g, 23%) as off white crystals: mp > 200 °C. $^1$H NMR (300 MHz, MeOD-$d_4$): δ 7.81–7.70 (m, 3H), 7.70–7.60 (m, 2H),

3.43 (d, $J$ = 12.3 Hz, 2H), 3.25–3.00 (m, 3H), 2.12–1.90 (m, 4H). $^{13}$C NMR (75 MHz, MeOD-$d_4$): δ 134.3, 132.5, 131.8, 131.4, 129.8, 129.4, 125.6, 125.3, 122.9, 45.1, 30.8, 30.7. Anal. calcd. ($C_{14}H_{18}N_4O \cdot 2HBr \cdot 1H_2O$): C, 38.38; H, 5.06; N, 12.79. Found: C, 38.50; H, 4.97; N, 12.30.

**3-(3-Azidophenyl)-4-(piperidin-4-yl)-1*H*-pyrazolol (2c).** In an amberized vial, **13a** (75 mg, 0.2 mmol) was dissolved in $CH_2Cl_2$ (6 mL) and carefully added TFA (1 mL) dropwise at rt. After 3.5 h, the reaction mixture was evaporated in vacuo and the resulting residue was lyophilized to afford compound **2c** (77 mg, 97%) as amorphous solid. $^1$H NMR (600 MHz, DMSO-$d_6$): δ 12.59 (b s, 1H), 8.76–8.62 (m, 1H), 8.50–8.35 (m, 1H), 7.60 (s, 1H), 7.48 (t, $J$ = 7.7 Hz, 1H), 7.41–7.39 (m, 1H), 7.24–7.23 (m, 1H), 7.09 (ddd, $J$ = 1.0, 2.4, 7.9 Hz, 1H), 3.34–3.29 (m, 2H), 3.06 (tt, $J$ = 3.5, 11.9 Hz, 1H), 3.03–2.96 (m, 2H), 1.99–1.93 (m, 2H), 1.67 (qd, $J$ = 3.9, 13.2 Hz, 2H). $^{13}$C NMR (150 MHz, DMSO-$d_6$): δ 158.2 (q, $J$ = 34.2 Hz, TFA), 139.7, 139.1, 135.5, 130.3, 123.9, 121.5, 120.2, 117.8, 117.4, 116.3 (q, $J$ = 295.4 Hz, TFA), 29.9, 29.4. HRMS (ESI-TOF): *m/z* calculated for $C_{14}H_{17}N_6O$ $[M + H]^+$, 285.1458. Found, 285.1465 (ΔM = 2.3 ppm). Purity by anal. HPLC (254 nm), 96%.

**5-(3-azidophenyl)-4-(piperidin-4-yl)-1*H*-pyrazol-1-ol (2d).** A suspension of **13b** (110 mg, 0.22 mmol) in EtOH/$Et_2O$ (1:1, 10 mL) was cooled to –78 °C where upon gaseous HCl was bubbled into the solution for one minute. After 5 minutes, the solution turned red and additional $Et_2O$ (10 mL) was added. The stirring was continued for 10 minutes (reaction was followed by TLC) before the solvents were removed *in vacuo*. Recrystallization from EtOH/$Et_2O$ afforded compound **2d** (34 mg, 55%) as amorphous solid. $^1$H NMR (300 MHz, $D_2O$): δ 7.34 (t, $J$ = 8.26Hz, 1H), 7.14 (s, 1H), 7.09–6.99 (m, 2H), 6.95 (m, 1H), 3.23 (d, $J$ = 12.7 Hz, 2H), 2.79 (td, $J$ = 2.3, 12.7 Hz, 2H), 2.67 (tt, $J$ = 3.7, 11.8 Hz, 1H), 1.81 (d, $J$ = 14.3 Hz, 2H), 1.61 (qd, $J$ = 4.1, 14.2 Hz,

2H). $^{13}$C NMR (75 MHz, $D_2O$): δ 140.8, 133.1, 130.6, 129.7, 129.5, 126.3, 121.2, 120.2, 112.0, 44.4, 29.8, 29.5. Purity by anal. HPLC, >99% (UV).

**2-azido-*N*-(2,76-dioxo-80-(2-oxohexahydro-1*H*-thieno[3,4-*d*]imidazol-4-yl)-6,9,12,15,18,21,24,27,30,33,36,39,42,45,48,51,54,57,60,63,66,69,72-tricosaoxa-3,75-diazaoctacontyl)-4-(1-hydroxy-4-(piperidin-4-yl)-1*H*-pyrazol-5-yl)benzamide (3b).** In an amberized vial and under an argon atmosphere, a solution of **20b** (258 mg, 0.15 mmol) in $CH_2Cl_2$ (3 mL) was added neat TFA (3 mL) dropwise. The resulting mixture was stirred for 1 h before it was evaporated *in vacuo*. Purification of the resulting residue by preparative HPLC (10–29% B, over 23 minutes) afforded compound **3b** (73 mg, 26%) as purple oil. 1.83 mg **3b** were dissolved in 492 µL methanol-$d_4$ (corresponding to a theoretical concentration of 2.0 mM) in a 1.7 mm NMR tube and used to quantification by ERETIC2. Using a 4.00 mM external reference sample of cinnamic acid in methanol-$d_4$, the concentration of **3b** was found to be 1.92 mM, translating to a molecular weight of **3b** of 1940.8 g/mol. $^1$H NMR (MeOD-$d_4$, 600 MHz): δ 7.97 (d, $J$ = 8.0 Hz, 1H), 7.46 (d, $J$ = 1.3 Hz, 1H), 7.40 (dd, $J$ = 8.0, 1.3 Hz, 1H), 7.27 (s, 1H), 4.50 (dd, $J$ = 7.8, 4.9 Hz, 1H), 4.31 (dd, $J$ = 7.8, 4.5 Hz, 1H), 4.11 (s, 2H), 3.64-3.61 (m, 88H), 3.60 (t, $J$ = 5.4 Hz, 2H), 3.54 (t, $J$ = 5.4 Hz, 2H), 3.45 (t, $J$ = 5.4 Hz, 2H), 3.44 (m, 2H), 3.36 (t, $J$ = 5.4 Hz, 2H), 3.20 (dt, $J$ = 9.6, 4.8 Hz, 1H), 3.07 (td, $J$ = 13.2, 2.3 Hz, 2H), 2.94 (m, 1H), 2.92 (dd, $J$ = 12.7, 5.0 Hz, 1H), 2.71 (d, $J$ = 12.7 Hz, 1H), 2.22 (t, $J$ = 7.3 Hz, 2H), 2.05 (br d, $J$ = 14.3 Hz, 2H), 1.84 (qd, $J$ = 13.4, 3.7 Hz, 2H), 1.74 (m, 1H), 1.67 (m, 2H), 1.61 (m, 1H), 1.44 (p, $J$ = 7.7 Hz, 2H). HRMS (ESI-TOF): *m/z* calculated for $C_{75}H_{134}N_{11}O_{28}S$ $[M + 3H]^{3+}$, 556.3935. Found, 556.3048 (ΔM = 2.5 ppm).

**2-azido-*N*-(2,76-dioxo-80-(2-oxohexahydro-1*H*-thieno[3,4-*d*]imidazol-4-yl)-6,9,12,15,18,21,24,27,30,33,36,39,42,45,48,51,54,57,60,63,66,69,72-tricosaoxa-3,75-**

**diazaoctacontyl)-4-(1-hydroxy-4-(piperidin-4-yl)-1*H*-pyrazol-3-yl)benzamide (3a).** In an amberized vial and under an argon atmosphere, a solution of **20a** (120 mg, 0.068 mmol) in $CH_2Cl_2$ (1.5 mL) was added neat TFA (1.5 mL) dropwise. The resulting mixture was stirred for 1 h before it was evaporated *in vacuo*. Purification of the resulting residue by preparative HPLC (0–50% B, over 10 minutes) afforded **3a** (112 mg, 88%) as purple oil. 1.26 mg of **3a** were dissolved in 339 µL methanol-$d_4$ (corresponding to a theoretical concentration of 2.0 mM) in a 1.7 mm NMR tube and used to quantification by ERETIC2. Using a 4.00 mM external reference sample of cinnamic acid in methanol-$d_4$, the concentration of **3a** was found to be 1.99 mM translating to a molecular weight of **3a** of 1872.1 g/mol. $^1$H NMR (MeOD-$d_4$, 600 MHz): δ 7.93 (d, $J$ = 8.0 Hz, 1H), 7.533 (s, 1H), 7.525 (d, $J$ = 1.3 Hz, 1H), 7.49 (dd, $J$ = 8.0, 1.3 Hz, 1H), 4.49 (dd, $J$ = 7.7, 4.8 Hz, 1H), 4.31 (dd, $J$ = 7.9, 4.5 Hz, 1H), 4.10 (s, 2H), 3.64-3.61 (m, 88H), 3.59 (t, $J$ = 5.4 Hz, 2H), 3.54 (t, $J$ = 5.4 Hz, 2H), 3.47 (m, 2H), 3.45 (t, $J$ = 5.4 Hz, 2H), 3.36 (t, $J$ = 5.4 Hz, 2H), 3.20 (dt, $J$ = 9.6, 4.8 Hz, 1H), 3.17 (m, 1H), 3.14 (td, $J$ = 13.1, 2.3 Hz, 2H), 2.93 (dd, $J$ = 12.7, 5.0 Hz, 1H), 2.71 (d, $J$ = 12.7 Hz, 1H), 2.22 (t, $J$ = 7.3 Hz, 2H), 2.16 (br d, $J$ = 14.0 Hz, 2H), 1.78 (qd, $J$ = 13.6, 3.7 Hz, 2H), 1.74 (m, 1H), 1.67 (m, 2H), 1.61 (m, 1H), 1.44 (p, $J$ = 7.7 Hz, 2H). HRMS (ESI-TOF): *m/z* calculated for $C_{75}H_{133}N_{11}O_{28}S$ $[M + 2H]^{2+}$, 833.9516. Found, 833.9518 (ΔM = 0.2 ppm).

**Methyl 4-(4-(3-benzoylphenyl)-3-isopropoxyisoxazol-5-yl)piperidine-1-carboxilate (5a).** A solution of **4** (0.19 g, 0.5 mmol) in DMF (3 mL) was added phenyl(3-(4,4,5,5-tetramethyl-1,3,2-dioxaborolan-2-yl)phenyl)methanone (0.3 g, 1.0 mmol), $Pd(PPh_3)_2Cl_2$ (34 mg, 0.05 mmol), $K_2CO_3$ (0.12 g, 1.0 mmol, in 1 mL of water). The resulting mixture was evacuated and purged with nitrogen six times and stirred at 70 °C for 19 h. Upon cooling to rt., $Et_2O$ (10 mL) was added and the organic phase was washed with water (10 mL), 2M NaOH (2 × 10 ml) and water (10 mL), dried over anhydrous $Na_2SO_4$, filtered, and evaporated *in vacuo*. Purification by FC

(Heptane/EtOAc, 0–100% EtOAc) afforded **5a** as yellow oil (0.17 g, 79%). $^{1}$H NMR (300 MHz, $CDCl_3$): δ 7.82–7.73 (m, 4H), 7.60–7.43 (m, 5H), 4.95 (heptet, *J* = 6.1 Hz, 1H), 4.17 (b s, 2H), 3.67 (s, 3H), 3.04–2.97 (m, 1H), 2.83–2.76 (m, 2H), 1.93–1.76 (m, 4H), 1.37 (d, *J* = 6.1 Hz, 6H). $^{13}$C NMR (300 MHz, $CDCl_3$): δ 195.9, 170.7, 168.2, 155.5, 137.7, 137.1, 132.4, 132.3, 130.2, 129.7, 128.83, 128.76, 128.6, 128.2, 105.8, 73.5, 52.6, 43.5, 34.5, 29.5, 22.0.

**Methyl 4-(4-(4-benzoylphenyl)-3-isopropoxyisoxazol-5-yl)piperidine-1-carboxylate (5b).** A solution of compound **4** (1.00 g, 2.5 mmol) in DMF (5 mL) was added (4-benzoylphenyl)boronic acid (1.14 g, 5.1 mmol), $Pd(PPh_3)_2Cl_2$ (0.12 g, 0.3 mmol), $K_2CO_3$ (0.65 g, 5.1 mmol in 2 mL of water). The resulting mixture was evacuated and purged with nitrogen six times and stirred at 70 °C for 19 h. Upon cooling to rt., $Et_2O$ (10 mL) was added and the organic phase was washed with water (10 mL), 2M NaOH (2 × 10 ml) and water (10 mL), dried over anhydrous $Na_2SO_4$, filtered, and evaporated in vacuo. Purification by FC (Heptane/EtOAc, 0–100% EtOAc) afforded **5a** as orange oil (0.60 g, 53%). $^{1}$H NMR (300 MHz, $CDCl_3$): δ 7.89–7.81 (m, 4H), 7.61–7.46 (m, 5H), 5.01 (heptet, *J* = 6.0 Hz, 1H), 4.23 (b s, 2H), 3.70 (s, 3H), 3.18–3.07 (m, 1H), 2.97–2.82 (m, 2H), 1.99–1.78 (m, 4H), 1.42 (d, *J* = 6.2 Hz, 6H). $^{13}$C NMR (300 MHz, $CDCl_3$): δ 195.4, 170.9, 168.0, 155.3, 137.0, 135.9, 132.9, 132.1, 130.1, 129.6, 128.1, 128.0, 105.7, 73.4, 52.4, 43.4, 34.4, 29.3, 21.8.

**Methyl 4-(4-(3-benzoylbenzyl)-3-isopropoxyisoxazol-5-yl)piperidine-1-carboxylate (6c).** Under a nitrogen atmosphere, a stirred solution of **4** (1.00 g, 2.5 mmol) in anhydrous THF (4 mL) was added $^{i}$PrMgCl (1.75M in THF, 1.45 mL) dropwise. The reaction mixture was allowed to warm to 0 °C and stirring was continued for 2 h before a solution of 3-benzoylbenzaldehyde[32] (0.53 g, 2.5 mmol) in anhydrous THF (3 mL) was added. The resulting reaction mixture was allowed to reach rt. and stirred overnight. The reaction mixture was quenched with saturated aq.

$NH_4Cl$ (2 mL) and $Et_2O$ (15 mL) was added and the phases were separated. The aq. phase was extracted with $Et_2O$ (2 × 15 mL) and the combined organic phases were dried over anhydrous $Na_2SO_4$, filtered, and evaporated *in vacuo*. Purification by FC (toluene/EtOAc, 5:1 followed by 2:1) afforded methyl 4-(4-((3-benzoylphenyl)(hydroxy)methyl)-3-isopropoxyisoxazol-5-yl)piperidine-1-carboxylate (0.35 g, 40%). $^1$H NMR (300 MHz, $CDCl_3$): δ 7.82 (s, 1H), 7.75–7.43 (m, 8H), 5.77 (s, 1H), 4.90–4.79 (m, 1H), 4.11 (b s, 2H), 3.67 (s, 3H), 3.18–2.56 (m, 3H), 1.86–1.47 (m, 4H), 1.31–1.26 (m, 6H). $^{13}$C NMR (300 MHz, $CDCl_3$): δ 196.1, 171.0, 168.1, 142.9, 137.0, 136.9, 132.2, 129.5, 129.4, 128.7, 127.9, 127.8, 127.0, 107.1, 73.2, 65.4, 52.4, 43.4, 34.3, 29.2, 28.9, 21.6. A solution of methyl 4-(4-((3-benzoylphenyl)(hydroxy)methyl)-3-isopropoxyisoxazol-5-yl)piperidine-1-carboxylate (0.40 g, 0.8 mmol) and $Et_3SiH$ (0.23 mL, 1.5 mmol) in $CH_2Cl_2$ (5 mL) was added TFA (1.8 mL) dropwise at rt. and the temperature was raised to 50 °C. After 2 h, the mixture was cooled to rt. and added water (5 ml). The aqueous phase was extracted with $Et_2O$ (3 × 15 ml) and the combined organic phases were dried over anhydrous $Na_2SO_4$, filtered and evaporated *in vacuo*. Purification by FC (Toluen/ EtOAc, 4:1) afforded **6c** as yellow oil (0.34 g, 87%). $^1$H NMR (300 MHz, $CDCl_3$): δ 7.65 (d, $J$ = 7.2 Hz, 1H), 7.64–7.49 (m, 5H), 7.48–7.34 (m, 2H), 7.29–7.27(m, 1H), 4.76 (heptet, $J$ = 6.1 Hz, 1H), 4.08 (b s, 2H), 3.59 (s, 3H), 2.74–2.67 (m, 3H), 1.73–1.58 (m, 4H), 1.29 (d, $J$ = 6.1 Hz, 6H). $^{13}$C NMR (300 MHz, $CDCl_3$): δ 195.9, 170.2, 169.4, 155.2, 139.3, 137.3, 137.1, 132.0, 131.7, 129.5, 129.3, 128.0, 127.9, 127.8, 102.8, 72.8, 52.3, 43.4, 34.2, 29.1, 26.5, 21.7.

**Methyl 4-(4-(4-benzoylbenzyl)-3-isopropoxyisoxazol-5-yl)piperidine-1-carboxylate (6d).** Under a nitrogen atmosphere, a stirred solution of **4** (1.00 g, 2.5 mmol) in anhydrous THF (4 mL) was added $^i$PrMgCl (1.75M in THF, 1.45 mL) dropwise. The reaction mixture was allowed to warm to 0 °C and stirring was continued for 2 h before a solution of 4-benzoylbenzaldehyde[33]

(0.53 g, 2.5 mmol) in anhydrous THF (3 mL) was added. The resulting reaction mixture was allowed to reach rt. and stirred overnight. The reaction mixture was quenched with saturated aq. $NH_4Cl$ (2 mL) and $Et_2O$ (15 mL) was added and the phases were separated. The aqueous phase was extracted with $Et_2O$ (2 × 15 mL) and the combined organic phases were dried over anhydrous $Na_2SO_4$, filtered, and evaporated *in vacuo*. Purification by FC (Petroleum Ether 40–65 °C/EtOAc, 0–100% EtOAc) afforded methyl 4-(4-((4-benzoylphenyl)(hydroxy)methyl)-3-isopropoxyisoxazol-5-yl)piperidine-1-carboxylate (0.36 g, 31%). $^1$H NMR (300 MHz, $CDCl_3$): δ 7.78–7.74 (m, 4H), 7.62–7.44 (m, 5H), 5.83 (s, 1H), 4.86 (heptet, *J* = 6.2 Hz, 1H), 4.12 (b s, 3H), 3.65 (s, 3H), 3.07–2.91 (m, 1H), 2.87–2.61 (m, 2H), 1.83–1.61 (m, 3H), 1.60–1.51 (m, 1H), 1.32 (d, *J* = 6.2 Hz, 6H). $^{13}$C NMR (300 MHz, $CDCl_3$): δ 196.1, 171.4, 168.4, 155.5, 147.1, 137.1, 136.3, 132.3, 129.9, 129.7, 128.1, 125.4, 107.0, 73.5, 65.5, 52.5, 43.5, 34.5, 29.4, 29.0, 21.9, 21.8. A solution of methyl 4-(4-(4-benzoylbenzyl)-3-isopropoxyisoxazol-5-yl)piperidine-1-carboxylate (0.30 g, 0.6 mmol) and $Et_3SiH$ (0.18 mL, 1.1 mmol) in $CH_2Cl_2$ (4 ml) was added TFA (1.4 mL) dropwise at rt. and the temperature was raised to 50 °C. After 2 h, the mixture was cooled to rt. and added water (5 mL). The aqueous phase was extracted with $Et_2O$ (3 × 15 ml) and the combined organic phases were dried over anhydrous $Na_2SO_4$, filtered and evaporated *in vacuo*. Purification by FC (Petroleum Ether 40–65 °C/EtOAc, 0–100% EtOAc) afforded **6d** as yellow oil (0.22 g, 76%). $^1$H NMR (300 MHz, $CDCl_3$): δ 7.74–7.69 (m, 4H), 7.54 (t, *J* = 7.2 Hz, 1H), 7.43 (t, *J* = 7.h Hz, 2H,), 7.25–7.23 (m, 2H), 4.85 (heptet, *J* = 6.1 Hz, 1H), 4.16 (b s, 2H), 3.68 (s, 2H), 3.66 (s, 3H), 2.88–2.72 (m, 3H), 1.87–1.62 (m, 4H), 1.32 (d, *J* = 6.1, 6H,). $^{13}$C NMR (300 MHz, $CDCl_3$): δ 195.9, 170.5, 169.7, 155.5, 144.0, 137.3, 135.5, 132.1, 130.2, 129.7, 128.0, 127.8, 102.6, 73.1, 52.6, 43.6, 34.5, 29.2, 26.8, 21.9.

***tert*-Butyl 4-(1-((4-methoxybenzyl)oxy)-1*H*-pyrazol-4-yl)piperidine-1-carboxylate (10b).** Under a nitrogen atmosphere, a solution of 4-iodo-1-benzyloxy-1*H*-pyrazole[36] (0.45 g, 1.5 mmol) in anhydrous THF (4 mL) was cooled to 0 °C and added isopropyl magnesium chloride (2M in THF, 0.9 mL, 1.8 mmol) dropwise. The mixture was stirred for 30 minutes at 0 °C before additional isopropyl magnesium chloride solution (0.9 mL, 1.8 mmol) was. The stirring was continued for additional 30 minutes before a solution of *tert*-butyl-4-oxo-piperidine-1-carboxylate (0.45 g, 2.3 mmol) in anhydrous THF (1.5 mL) was slowly added. The resulting mixture was stirred over-night before a saturated aqueous solution of $NH_4Cl$ (4 mL) was added. The aqueous phase was extracted with $Et_2O$ (3 × 5 mL) and the combined organic layer was dried over $MgSO_4$, filtered, and evaporated *in vacuo*. The resulting residue was dissolved in EtOH (20 mL) and added Pd/C (10% w/w, 50 mg). The flask was evacuated and refilled with hydrogen six times and allowed to stir for 24 h before the reaction mixture was filtered through a plug of celite. The filtrate was collected and evaporated *in vacuo*. Purification by DCVC (EtOAc/Heptane, 0–100% EtOAc) afforded *tert*-butyl 4-(1-hydroxy-1*H*-pyrazol-4-yl)piperidine-1-carboxylate as clear oil, which was re-dissolved in acetone and cooled to 0 °C. *para*-Methoxybenzyl chloride (0.30 mL, 2.2 mmol) and potassium carbonate (0.31 g, 2.2 mmol) was added and the resulting mixture was allowed to stir at rt. over-night before the mixture was filtered and evaporated *in vacuo*. Purification by DCVC (EtOAc/Heptane, 0–100% EtOAc) afforded **10b** as clear oil (0.22 g, 38%). $^1$H NMR (300 MHz, $CDCl_3$): δ 7.17 (d, $J$ = 8.2 Hz, 2H), 7.08 (d, $J$ = 0.5 Hz, 1H), 6.84 (d, $J$ = 8.1 Hz, 2H), 6.73 (d, $J$ = 0.6 Hz, 1H), 5.20 (s, 2H), 4.07 (d, $J$ = 11.4 Hz, 2H) 3.81 (3H, s), 2.77 (t, $J$ = 12.6 Hz, 2H) 2.52 (tt, $J$ = 3.8, 11.6 Hz, 1H), 1.77 (d, $J$ = 12.5 Hz, 2H), 1.47 (s, 9H), 1.38 (dd, $J$ = 4.0, 12.5 Hz, 1H).

***tert*-Butyl 4-(5-iodo-1-((4-methoxybenzyl)oxy)-1*H*-pyrazol-4-yl)piperidine-1-carboxylate (10e).** Under a nitrogen atmosphere, a cooled solution (–78 °C) of lithium diisopropylamide (1M

in THF, 0.34 mL, 0.34 mmol) in THF (0.67 mL) was added a solution of **10b** (0.11 g, 0.3 mmol) in anhydrous THF (1 mL) dropwise. After 10 minutes of stirring at –78 °C, a solution of iodine (0.22 g, 0.9 mmol) in anhydrous THF (2 mL) was added and the resulting solution was allowed to reach rt. slowly over-night. The reaction was quenched with a saturated aqueous solution of $Na_2SO_3$ (8 mL) and the aqueous phase was extracted with EtOAc (3 × 10 mL) and the combined organic phases were dried over $MgSO_4$, filtered, and evaporated *in vacuo*. Purification by DCVC (EtOAc/Heptane, 0–100% EtOAc) afforded **10e** as clear oil (65 mg, 45%). $^1$H NMR (300 MHz, $CDCl_3$): δ 7.31 (d, *J* = 8.7 Hz, 2H), 7.17 (s, 1H), 6.87 (d, *J* = 8.7 Hz, 2H), 5.19 (s, 2H) 4.18 (d, *J* = 11.9 Hz, 2H), 3.81 (s, 3H), 2.77 (t, *J* = 12.8 Hz, 2H), 2.57 (tt, *J* = 3.8, 12.2 Hz, 1H), 1.78 (d, *J* = 11.1 Hz, 2H), 1.60–1.44 (m, 11H).

***tert*-Butyl 4-(1-(benzyloxy)-3-iodo-1*H*-pyrazol-4-yl)piperidine-1-carboxylate (10f).** A suspension of methyl 4-(1-(benzyloxy)-3-iodo-1*H*-pyrazol-4-yl)piperidine-1-carboxylate (**10c**)[14] (7.04 g, 16.0 mmol) and KOH (17.9 g, 319 mmol) in water/MeOH (1:3, 280 mL) was stirred at reflux for 24 h. Upon cooling to rt., the MeOH was removed *in vacuo*, and the remaining aqueous phase was extracted with $Et_2O$ (1 L) by continues extraction using a Kutchel-Stüdel apparatus over-night. The resulting organic phase was dried over $MgSO_4$, filtered, and evaporated *in vacuo* to give the crude 4-(1-(benzyloxy)-3-iodo-1*H*-pyrazol-4-yl)piperidine (3.97 g) as clear oil, which was used without further purification. Under a nitrogen atmosphere, 4-(1-(benzyloxy)-5-iodo-1*H*-pyrazol-4-yl)piperidine was re-dissolved in $CH_2Cl_2$ (200 mL) and solution was added $Et_3N$ (2.9 mL, 20.7 mmol) and di-*tert*-butyl dicarbonate (4.52 g, 20.7 mmol). The resulting mixture was stirred over night before it was quenched with water (500 mL). The phases were separated and the organic phase was washed with 1N aq. HCl (200 mL), water (200 mL) and Brine (200 mL), dried over $MgSO_4$, filtered, and evaporated *in vacuo*. Purification by CC (Pet. Ether 40–65 °C/EtOAc,

8:2) afforded **10f** (3.93 g, 51% over two steps) as clear oil. $^1$H NMR (600 MHz, $CDCl_3$): δ 7.39–7.33 (m, 3H), 7.29–7.26 (m, 2H), 6.57 (s, 1H), 5.25 (s, 2H), 4.13 (b s, 2H), 2.75 (m, 2H), 2.37 (tt, *J* = 3.5, 12.0 Hz, 1H), 1.77 (b d, *J* = 13.0 Hz, 2H), 1.46 (s, 9H), 1.28-1.20 (m, 2H). $^{13}$C NMR (150 MHz, $CDCl_3$): δ 154.9, 133.6, 129.9, 129.6, 128.8, 128.0, 121.3, 90.1, 81.2, 79.7, 44.1, 34.7, 32.5, 28.6.

***tert*-Butyl 4-(1-(benzyloxy)-5-iodo-1*H*-pyrazol-4-yl)piperidine-1-carboxylate (10g).** A suspension of methyl 4-(1-(benzyloxy)-5-iodo-1*H*-pyrazol-4-yl)piperidine-1-carboxylate (**10d**)[14] (4.32 g, 9.8 mmol) and KOH (16.5 g, 294 mmol) in water/MeOH. (1:1, 300 mL) was stirred at reflux for 24 h. Upon cooling to rt., the MeOH was removed *in vacuo*, and the remaining aqueous phase was extracted with $Et_2O$ (1 L) by continues extraction using a Kutchel-Stüdel apparatus over-night. The resulting organic phase was dried over $MgSO_4$, filtered, and evaporated *in vacuo* to give the crude 4-(1-(benzyloxy)-5-iodo-1*H*-pyrazol-4-yl)piperidine (3.52 g) as clear oil, which was used without further purification. $^1$H NMR (600 MHz, $CDCl_3$): δ 7.45–7.36 (m, 5H), 7.23 (s, 1H), 5.27 (s, 2H), 4.74 (b s, 2H), 3.17–3.13 (m, 2H), 2.71 (dt, *J* = 2.2, 12.3 Hz, 2H), 2.42 (tt, *J* = 3.4, 12.2 Hz, 1H), 1.80 (b d, *J* = 12.9 Hz, 2H), 1.55 (dq, *J* = 3.6, 12.7 Hz, 2H). Under a nitrogen atmosphere, 4-(1-(benzyloxy)-5-iodo-1*H*-pyrazol-4-yl)piperidine was re-dissolved in $CH_2Cl_2$ (200 mL) and solution was added $Et_3N$ (2.73 mL, 19.6 mmol) and di-*tert*-butyl dicarbonate (4.28 g, 16.6 mmol). The resulting mixture was stirred over night before it was quenched with water (300 mL). The phases were separated and the organic phase was washed with 1N aq. HCl (200 mL), water (200 mL) and Brine (200 mL), dried over $MgSO_4$, filtered, and evaporated *in vacuo*. Purification by CC (Pet. Ether 40–65 °C/EtOAc, 8:2) afforded **10g** (4.00 g, 84% over two steps) as clear oil, which solidified over time: mp 71–73 °C. $^1$H NMR (600 MHz, $CDCl_3$): δ 7.44–7.36 (m, 5H), 7.20 (s, 1H), 5.27 (s, 2H), 4.19 (b s, 2H), 2.78 (d t, *J* = 13.0 Hz, 2H), 2.44 (tt, *J* = 3.8,

12.2 Hz, 1H), 1.78 (b d, *J* = 13.5 Hz, 2H), 1.53 (dq, *J* = 4.5, 12.9 Hz, 2H), 1.48 (s, 9H). $^{13}$C NMR (150 MHz, $CDCl_3$): δ 154.9, 133.2, 132.0, 130.2, 129.6, 128.7, 128.0, 81.1, 79.7, 75.5, 44.2, 34.4, 32.2, 28.6.

**Ethyl 4-(3-(3-aminophenyl)-1-(benzyloxy)-1*H*-pyrazol-4-yl)piperidine-1-carboxylate (11a).** Under a nitrogen atmosphere, **10c**[14] (0.50 g, 1.1 mmol) in anhydrous DMF (5.5 mL) was added 3-aminophenylboronic acid hydrochloride (0.38 g, 2.2 mmol) and $K_2CO_3$ (0.46 g, 3.3 mmol, in 1.30 mL $H_2O$). The resulting solution was purged with nitrogen for 3 minutes, added $Pd(PPh_3)_2Cl_2$ (38 mg, 0.06 mmol), and purged with nitrogen for additional 3 minutes. The resulting reaction mixture was stirred vigorously at 90 °C for 25 h. Upon cooling to rt., water (50 mL) and $Et_2O$ (50 mL) was added and the phases were separated. The organic phase was washed with 1M aq. NaOH (2 × 50 mL) and water (50 mL), dried over $MgSO_4$, filtered, and evaporated *in vacuo*. Purification by CC (heptane/EtOAc, 1:1) resulted in **11a** (0.39 g, 83%) as viscous clear oil. $^1$H NMR (400 MHz, $CDCl_3$): δ 7.39–7.22 (m, 5H), 7.20 (t, *J* = 7.7 Hz, 1H), 6.95–6.90 (m, 2H), 6.77 (d, *J* = 0.5 Hz, 1H), 6.68 (ddd, *J* = 8.1, 2.4, 1.0 Hz, 1H), 5.29 (s, 2H), 4.14 (b s, 2H), 4.12 (q, *J* = 7.1 Hz, 2H), 3.72 (b s, 2H), 2.85–2.72 (m, 3H), 1.81–1.74 (b d, *J* = 13.2 Hz, 2H), 1.34–1.23 (m, 2H), 1.25 (t, J = 7.1 Hz, 3H). $^{13}$C NMR (150 MHz, $CDCl_3$): δ 155.5, 146.8, 143.2, 134.6, 133.9, 129.7, 129.4, 129.2, 128.6, 121.2, 121.1, 118.2, 114.7, 114.5, 80.5, 61.2, 44.2, 33.5, 32.0, 14.7.

**Ethyl 4-(5-(3-aminophenyl)-1-(benzyloxy)-1*H*-pyrazol-4-yl)piperidine-1-carboxylate (11b).** Under a nitrogen atmosphere, **10d**[14] (4.62 g, 10.1 mmol) in anhydrous DMF (50 mL) was added 3-Aminophenylboronic acid (2.74 g, 15.5 mmol) and $K_2CO_3$ (2.82 g, 20.4 mmol, in 6.8 mL $H_2O$). The resulting solution was purged with nitrogen for 3 minutes, added $Pd(PPh_3)_2Cl_2$ (0.75 g, 1.1 mmol), and purged with nitrogen for additional 3 minutes. The resulting reaction mixture was stirred vigorously at 90 °C for 25 h. Upon cooling to rt., water (200 mL) and $Et_2O$ (300 mL) was

added and the phases were separated. The organic phase was washed with 1M aq. NaOH (2 × 200 mL) and water (200 mL), dried over $MgSO_4$, filtered, and evaporated *in vacuo*. Purification by CC (heptane/EtOAc, 1:1) resulted in **11b** (385 mg, 83%) as viscous clear oil. $^1$H NMR (300 MHz, $CDCl_3$): δ 7.33–7.12 (m, 5H), 7.07–7.01 (m, 2H), 6.07 (t, *J* = 2.3, 8.2 Hz, 1H), 6.57 (d, *J* = 7.6 Hz, 1H), 6.44 (t, *J* = 1.8 Hz, 1H), 5.06 (s, 2H), 4.13 (q, *J* = 7.0 Hz, 4H), 3.71 (s, 2H), 2.72 (t, *J* = 12.3 Hz, 2H), 2.59 (tt, *J* = 3.5, 12.3 Hz, 1H), 1.72 (d, *J* = 12.3 Hz, 2H), 1.55 (qd, *J* = 4.1, 12.3 Hz, 2H), 1.27 (t, *J* = 7.0 Hz, 3H). $^{13}$C NMR (75 MHz, $CDCl_3$): δ 155.6, 146.4, 133.6, 133.2, 130.2, 130.0, 129.4, 129.2, 129.0, 128.4, 121.5, 119.8, 116.1, 115.3, 80.4, 61.4, 44.3, 33.4, 32.2, 14.9.

***tert*-Butyl 4-(3-(3-aminophenyl)-1-(benzyloxy)-1*H*-pyrazol-4-yl)piperidine-1-carboxylate (11c).** Under an argon atmosphere, a MW reactor vial was charged with **10f** (0.48 g, 1.0 mmol), 3-aminophenylboronic acid (0.44 g, 2 mmol), $K_2CO_3$ (0.42 g, 3.0 mmol), DMF (6 mL), and water (3 mL). The resulting suspension was purged with argon for 10 minutes, added $Pd(PPh_3)_4$ (0.12 g, 0.1 mmol), and purged with argon for additional 5 minutes before the vial was sealed and heated at 90 °C (conventional heating) over-night. Upon cooling to rt., the crude mixture was added water (25 mL) and $CH_2Cl_2$ (25 mL) and the phases were separated. The aqueous phase was extracted with $CH_2Cl_2$ (3 × 25 mL). The combined organic phases were dried over $MgSO_4$, filtered, and evaporated *in vacuo*. Purification by CC (Pet. Ether 40–65 °C/EtOAc, 8:2) afforded **11c** (0.33 g, 73%) as yellow oil. $^1$H NMR (600 MHz, $CDCl_3$): δ 7.38–7.34 (m, 3H), 7.32–7.29 (m, 2H), 7.19 (t, *J* = 7.7 Hz, 1H), 6.96–6.93 (m, 1H), 6.93–6.91 (m, 1H), 6.78 (s, 1H), 6.68 (ddd, *J* = 0.9, 2.4, 8.0 Hz, 1H), 5.29 (s, 2H), 4.09 (b s, 2H), 3.72 (b s, 2H), 2.78 (tt, *J* = 3.6, 12.0 Hz, 1H), 2.74–2.64 (m, 2H), 1.76 (b d, *J* = 12.8 Hz, 2H), 1.45 (s, 9H), 1.32–1.23 (m, 2H). $^{13}$C NMR (150 MHz, $CDCl_3$): δ 155.0, 146.8, 143.8, 143.3, 134.8, 134.1, 129.9, 129.5, 129.4, 128.7, 121.34, 121.31, 118.5, 114.9, 114.6, 80.7, 79.5, 44.3, 33.8, 32.3, 28.6.

***tert*-Butyl 4-(5-(3-aminophenyl)-1-((4-methoxybenzyl)oxy)-1*H*-pyrazol-4-yl)piperidine-1-carboxylate (11d).** Under an argon atmosphere, a flask was charged with compound **10e** (0.25 g, 0.5 mmol), 3-aminophenylboronic acid hydrochloride (0.13 g, 0.7 mmol), $K_2CO_3$ (0.42 g, 3.0 mmol), DMF (3 mL), and $K_2CO_3$ (3M in water, 0.5 mL, 1.5 mmol). The resulting suspension was purged with argon for 10 minutes, added $Pd(PPh_3)_2Cl_2$ (34 mg, 0.05 mmol), and purged with argon for additional 5 minutes before being heated at 90 °C over-night. Upon cooling to rt., the crude mixture was added $Et_2O$ (20 mL) and the organic phase was washed with water (10 mL), aq. NaOH (2.5M, 2 × 10 mL) and water (10 mL), dried over $MgSO_4$, filtered, and evaporated *in vacuo*. Purification by DCVC (EtOAc/Heptane, 0–100% EtOAc) afforded **11d** (190 mg, 83%) as clear oil. $^1$H NMR (300 MHz, $CDCl_3$): δ 7.17 (s, 1H), 7.16 (t, *J* = 7.8 Hz, 1H), 6.93 (d, *J* = 8.6 Hz, 2H), 6.72 (m, 3H), 6.59 (dd, *J* = 1.2, 7.6 Hz, 1H), 6.47 (s, 1H), 4.99 (s, 2H), 4.13 (s, 2H), 3.79 (s, 3H), 2.67 (t, *J* = 12.9 Hz, 2H), 2.57 (tt, *J* = 4.1, 11.9 Hz, 1H), 1.71 (d, *J* = 12.6 Hz, 2H), 1.62–1.42 (m, 11H). $^{13}$C NMR (75 MHz, $CDCl_3$): δ 160.5, 155.2, 146.7, 133.6, 132.0, 130.5, 129.61, 129.57, 126.0, 121.8, 120.0, 116.4, 115.5, 114.0, 80.4, 79.8, 55.7, 44.6, 33.7, 32.6, 28.9.

***tert*-Butyl 4-(3-(3-aminophenyl)-1-hydroxy-1*H*-pyrazol-4-yl)piperidine-1-carboxylate (12).** Compound **11c** (0.26 g, 0.6 mmol) was dissolved in MeOH (10 mL) and added Pd/C (10% w/w, 25 mg). The flask was evacuated and refilled with hydrogen six times and allowed to stir for 1.5 h before the reaction mixture was filtered through a plug of celite. The filtrate was collected and evaporated *in vacuo* to afford **12** (0.20 g, 99%) as sticky solid. $^1$H NMR (600 MHz, DMSO-$d_6$): δ 12.20 (b s, 1H), 7.51 (b s, 1H), 7.03 (t, *J* = 7.8 Hz, 1H), 6.76–6.74 (m, 1H), 6.66–6.64 (m, 1H), 6.50 (ddd, *J* = 1.0, 2.4, 7.9 Hz, 1H), 5.08 (b s, 2H), 4.05–3.95 (m, 2H), 2.79 (tt, *J* = 3.5, 12.0 Hz, 1H), 2.75 (b s, 2H), 1.80–1.72 (m, 2H), 1.40 (s, 9H), 1.37 (dq, *J* = 4.0, 12.6 Hz, 2H). $^{13}$C NMR

(150 MHz, DMSO-$d_6$): δ 153.8, 148.6, 140.9, 134.5, 128.8, 121.2, 120.7, 115.1, 113.1, 112.7, 78.5, 43.3, 33.4, 31.8, 28.1.

***tert*-Butyl 4-(3-(3-azidophenyl)-1-hydroxy-1*H*-pyrazol-4-yl)piperidine-1-carboxylate (13a).** In an amberized vial and under an argon atmosphere, a suspension of **12** (149 mg, 0.4 mmol) in anhydrous acetonitrile (5 mL) was cooled to 0 °C and added first TMS-$N_3$ (0.066 mL, 0.5 mmol) followed by *tert*-butyl nitrite (0.074 mL, 0.6 mmol) dropwise. The resulting mixture was allowed to reach rt. and stirred over-night. The volatiles were removed *in vacuo* and purification by CC (EtOAc) of the resulting residue afforded **13a** (76 mg, 48%) as sticky oil. $^1$H NMR (600 MHz, DMSO-$d_6$): δ 12.43 (s, 1H), 7.61 (s, 1H), 7.46 (t, $J$ = 7.8 Hz, 1H), 7.37 (ddd, $J$ = 0.9, 1.4, 7.7 Hz, 1H), 7.21–7.20 (m, 1H), 7.06 (ddd, $J$ = 0.9, 2.3, 7.9 Hz, 1H), 4.00 (b s, 2H), 2.83 (tt, $J$ = 3.4, 11.8 Hz, 1H), 2.76 (b s, 2H), 1.81–1.74 (m, 2H), 1.41 (dq, $J$ = 4.2, 12.8 Hz, 2H), 1.40 (s, 9H). $^{13}$C NMR (150 MHz, DMSO-$d_6$): δ 153.8, 139.6, 139.0, 135.7, 130.3, 123.9, 121.8, 121.4, 117.7, 117.3, 78.5, 43.7, 33.3, 31.8, 28.0.

***tert*-butyl 4-(5-(3-azidophenyl)-1-((4-methoxybenzyl)oxy)-1*H*-pyrazol-4-yl)piperidine-1-carboxylate (13b).** Protected from light and under an argon atmosphere, a solution of **11d** (90 mg, 0.2 mmol) in acetonitrile (4 mL) was cooled to 0 °C and added first TMS-$N_3$ (0.03 mL, 0.23 mmol) followed by *tert*-butyl nitrite (0.03 mL, 0.28 mmol) dropwise. The cooling bath was removed and the reaction was stirred 1 h at rt. before the solvent was removed *in vacuo*. Purification by DCVC (EtOAc/Heptane, 0–100% EtOAc) afforded **13b** (78 mg, 82%) as clear oil. $^1$H NMR (300 MHz, $CDCl_3$): δ 7.33–7.29 (m, 2H), 7.21 (s, 1H), 7.00 (ddd, $J$ = 1.1, 2.3, 8.1 Hz, 1H), 6.92 (ddd, $J$ = 1.0, 1.6, 7.7 Hz, 1H), 6.81 (d, $J$ = 8.8 Hz, 2H), 6.65 (d, $J$ = 8.8 Hz, 2H), 5.20 (s, 2H), 4.21 (s, 2H), 3.82 (s, 3 H), 2.79 (t, $J$ = 12.8 Hz, 2H), 2.45 (tt, $J$ = 3.7, 12.0 Hz, 1H), 1.79 (d, $J$ = 13.2 Hz, 2H), 1.59–

1.50 (m, 11H). $^{13}$C NMR (75 MHz, $CDCl_3$): δ 160.5, 155.1, 140.3, 132.7, 131.9, 130.8, 130.4, 129.9, 126.3, 125.7, 121.9, 120.0, 119.0, 113.9, 80.5, 79.9, 55.7, 44.2, 33.8, 32.7, 29.0.

**Benzyl (4-bromo-2-nitrobenzoyl)glycinate (15).** In a flame-dried flask, a solution of 4-bromo-2-nitrobenzoic acid (**14**, 10.0 g, 41.3 mmol) in DMF (60 mL) at 0 °C was added carbonyldiimidazole (7.21 g, 43.3 mmol), under a nitrogen atmosphere, and stirred for 100 minutes. Then, glycine benzyl ester hydrochloride (8.75 g, 43.3 mmol) was added and the resulting mixture was allowed to reach rt. and stirred over-night. Water (200 mL) was added and the resulting precipitate was isolated by filtration off and dried to afford **15** (13.4 g, 83%) as white solid: mp 149–151 °C. $^1$H NMR (600 MHz, $CDCl_3$): δ 8.81 (d, $J$ = 1.9 Hz, 1H), 7.80 (dd, $J$ = 1.9, 8.1 Hz, 1H), 7.43 (d, $J$ = 8.1 Hz, 1H), 7.40–7.33 (m, 5H), 6.42–6.36 (m, 1H), 5.23 (s, 2H), 4.28 (d, $J$ = 5.1 Hz, 2H). $^{13}$C NMR (600 MHz, $CDCl_3$): δ 169.4, 165.6, 147.2, 136.8, 135.0, 131.0, 130.2, 128.9, 128.7, 127.9, 124.5, 67.8, 42.1.

**Benzyl (2-nitro-4-(4,4,5,5-tetramethyl-1,3,2-dioxaborolan-2-yl)benzoyl)glycinate (16).** Under an argon atmosphere, a flame-dried MW reactor vial was charged with **15** (1.00 g, 2.5 mmol), bis(pinacolato)diboron (0.71 g, 2.8 mmol), potassium acetate (0.74 g, 7.5 mmol), and anhydrous 1,4-dioxane (20 mL). The resulting suspension was purged with argon for 10 minutes, added $Pd(dppf)Cl_2 \cdot CH_2Cl_2$ (65 mg, 0.08 mmol), and purged with argon for additional 2 minutes before the vial was sealed and heated at 100 °C (conventional heating) for 2 h. HPLC analysis showed full conversion of **15** and formation of only one new product. Upon cooling to rt., the crude mixture was filtered through a plug of celite and the filtrate was evaporated *in vacuo*. The resulting residue was suspended in water (50 mL) and extracted with $CH_2Cl_2$ (3 × 50 mL). The combined organic phases were dried over $MgSO_4$, filtered, and evaporated *in vacuo* to give the crude **16** as black tar (1.34 g, 120%), which was used without further purification. $^1$H NMR (600

MHz, $CDCl_3$): δ 8.44 (d, *J* = 0.8 Hz, 1H), 8.05 (dd, *J* = 1.1, 7.5 Hz, 1H), 7.53 (d, *J* = 7.5 Hz, 1H), 7.40–7.34 (m, 5H), 6.37 (b t, *J* = 4.9 Hz, 1H), 5.23 (s, 2H), 4.30 (d, *J* = 4.9 Hz, 2H), 1.36 (s, 12H). $^{13}$C NMR (150 MHz, $CDCl_3$): δ 169.6, 166.5, 146.3, 139.9, 135.1, 134.2, 130.6, 128.9, 128.8, 128.6, 128.2, 85.0, 67.7, 67.2, 42.1, 25.0.

**(4-(1-(Benzyloxy)-4-(1-(*tert*-butoxycarbonyl)piperidin-4-yl)-1*H*-pyrazol-3-yl)-2-nitrobenzoyl)glycine (17a).** Under an argon atmosphere, a MW reactor vial was charged with **10f** (0.48 g, 1.0 mmol), crude **16** (2.5 mmol), $K_2CO_3$ (0.41 g, 3.0 mmol), DMF (12 mL), and water (6 mL). The resulting suspension was purged with argon for 10 minutes, added $Pd(PPh_3)_4$ (0.12 g, 0.1 mmol), and purged with argon for additional 5 minutes before the vial was sealed and heated at 90 °C over-night. Upon cooling to rt., the crude mixture was filtered through a plug of celite and the filtrate was evaporated *in vacuo*. Purification by preparative HPLC (50–80% B, over 15 mL/min) afforded **17a** (0.312 g, 54%) as sticky oil. $^1$H NMR (600 MHz, DMSO-*d*$_6$): δ 12.75 (b s, 1H), 9.07 (t, *J* = 5.8 Hz, 1H), 8.12 (d, *J* =1.7 Hz, 1H), 7.99 (dd, *J* = 1.7, 8.0 Hz, 1H), 7.72 (s, 1H), 7.71 (d, *J* = 8.0 Hz, 1H), 7.45–7.39 (m, 5H), 5.35 (s, 2H), 4.02–3.92 (m, 2H), 3.94 (d, *J* = 5.8 Hz, 2H), 2.89 (tt, *J* = 3.3, 12.0 Hz, 1H), 2.78 (b s, 2H), 1.76 (b d, *J* = 12.5 Hz, 2H), 1.40 (s, 9H), 1.32 (qd, *J* = 4.0, 12.8 Hz, 2H). $^{13}$C NMR (150 MHz, DMSO-*d*$_6$): δ 170.8, 165.3, 153.8, 147.6, 138.6, 135.9, 133.7, 131.4, 130.1, 129.71, 129.66, 129.1, 128.5, 122.9, 122.4, 122.3, 80.4, 78.6, 43.5, 41.1, 32.9, 31.5, 28.1. HRMS (ESI-TOF): *m/z* calculated for $C_{29}H_{34}N_5O_8$ $[M + H]^+$, 580.2388. Found, 580.2397 (ΔM = 0.9 ppm).

**(4-(1-(Benzyloxy)-4-(1-(*tert*-butoxycarbonyl)piperidin-4-yl)-1*H*-pyrazol-5-yl)-2-nitrobenzoyl)glycine (17b).** Under an argon atmosphere, a MW reactor vial was charged with **10g** (0.97 g, 2.0 mmol), crude **16** (2.6 g, 5 mmol), $K_2CO_3$ (0.83 g, 6.0 mmol), DMF (12 mL), and water (6 mL). The resulting suspension was purged with argon for 10 minutes, added $Pd(PPh_3)_4$ (0.23 g,

0.2 mmol), and purged with argon for additional 5 minutes before the vial was sealed and heated at 90 °C (conventional heating) over-night. Upon cooling to rt., the crude mixture was filtered through a plug of celite and the filtrate was evaporated *in vacuo*. Purification by preparative HPLC (50–72% B, over 12 mL/min) afforded **17b** (0.66 g, 49%) as sticky oil. $^{1}$H NMR (600 MHz, DMSO-$d_6$): δ 12.76 (b s, 1H), 9.11 (t, $J$ = 5.8 Hz, 1H), 7.65 (d, $J$ = 7.9 Hz, 1H), 7.64 (d, $J$ = 1.5 Hz, 1H), 7.61 (dd, $J$ = 1.5, 7.8 Hz, 1H), 7.48 (s, 1H), 7.30–7.26 (m, 1H), 7.22–7.18 (m, 2H), 7.02–6.98 (m, 2H), 5.19 (s, 2H), 3.97 (b s, 2H), 3.96 (t, $J$ = 5.8 Hz, 2H), 2.68 (b s, 2H), 2.53 (tt, $J$ = 3.6, 11.9 Hz, 1H), 1.64 (b d, $J$ = 12.4 Hz, 2H), 1.45 (qd, $J$ = 4.2, 12.6 Hz, 2H), 1.39 (s, 9H). $^{13}$C NMR (150 MHz, DMSO-$d_6$): δ 170.7, 165.2, 153.7, 147.1, 133.7, 133.0, 131.1, 130.8, 130.1, 130.0, 129.8, 129.4, 129.1, 128.2, 124.2, 122.2, 79.9, 78.6, 43.6, 41.0, 32.7, 31.3, 28.1. HRMS (ESI-TOF): *m/z* calculated for $C_{29}H_{34}N_5O_8$ $[M + H]^+$, 580.2402. Found, 580.2389 (ΔM = 2.2 ppm).

**(2-Amino-4-(4-(1-(*tert*-butoxycarbonyl)piperidin-4-yl)-1-hydroxy-1*H*-pyrazol-3-yl)benzoyl)glycine (18a).** Compound **17a** (0.31 g, 0.5 mmol) was dissolved in DMF (10 mL) and added Pd/C (10% w/w, 31 mg). The flask was evacuated and refilled with hydrogen six times and allowed to stir for 3 h before the reaction mixture was filtered through a plug of celite. The filtrate was collected and evaporated *in vacuo* to afford **18a** (0.24 g, 98%) as sticky solid. $^{1}$H NMR (600 MHz, DMSO-$d_6$): δ 12.46 (b s, 2H), 8.49 (t, $J$ = 5.8 Hz, 1H), 7.56 (s, 1H), 7.55 (d, $J$ = 8.4 Hz, 1H), 6.91 (d, $J$ = 1.7 Hz, 1H), 6.71 (dd, $J$ = 1.7, 8.2 Hz, 1H), 6.55 (b s, 2H), 4.07–3.95 (m, 2H), 3.85 (d, $J$ = 5.8 Hz, 2H), 2.88–2.81 (m, 1H), 2.77 (b s, 2H), 1.82–1.75 (m, 2H), 1.40 (s, 9H), 1.38 (qd, $J$ = 3.5, 12.1 Hz, 2H). $^{13}$C NMR (150 MHz, DMSO-$d_6$): δ 171.5, 168.8, 153.8, 149.9, 139.7, 137.3, 128.3, 121.5, 121.4, 114.9, 113.8, 112.4, 78.5, 43.8, 41.0, 33.2, 31.8, 28.1.

**(2-Amino-4-(4-(1-(*tert*-butoxycarbonyl)piperidin-4-yl)-1-hydroxy-1*H*-pyrazol-5-yl)benzoyl)glycine (18b).** Compound **17b** (0.66 g, 1.0 mmol) was dissolved in DMF (6 mL) and

added Pd/C (10% w/w, 66 mg). The flask was evacuated and refilled with hydrogen six times and allowed to stir for 3 h before the reaction mixture was filtered through a plug of celite. The filtrate was evaporated *in vacuo* to afford **18b** (0.45 g, quant.) as brown oil. $^{1}$H NMR (600 MHz, DMSO-$d_6$): δ 12.41 (b s, 2H), 8.58 (t, $J$ = 5.8 Hz, 1H), 7.60 (d, $J$ = 8.3 Hz, 1H), 7.15 (s, 1H), 6.80 (d, $J$ = 1.4 Hz, 1H), 6.61 (dd, $J$ = 1.4, 8.3 Hz, 1H), 6.58 (b s, 2H), 4.04–3.92 (m, 2H), 3.87 (d, $J$ = 5.8 Hz, 2H), 2.69 (b s, 2H), 2.60 (tt, $J$ = 3.5, 8.3 Hz, 1H), 1.72–1.65 (m, 2H), 1.42 (qd, $J$ = 4.3, 12.8 Hz, 2H), 1.39 (s, 9H). $^{13}$C NMR (150 MHz, DMSO-$d_6$): δ 171.5, 168.7, 153.8, 149.6, 132.0, 131.1, 128.6, 128.2, 121.3, 117.0, 115.6, 113.4, 78.5, 43.7, 41.0, 33.0, 31.7, 28.1. HRMS (ESI-TOF): *m/z* calculated for $C_{22}H_{30}N_5O_6$ $[M + H]^+$, 460.2191. Found, 460.2178 (ΔM = 2.8 ppm).

**(2-Azido-4-(4-(1-(*tert*-butoxycarbonyl)piperidin-4-yl)-1-hydroxy-1*H*-pyrazol-3-yl)benzoyl)glycine (19a).** In an amberized flask and under an argon atmosphere, a suspension of **18a** (0.24 g, 0.5 mmol) in anhydrous acetonitrile (30 mL) and THF (20 mL) was cooled to 0 °C and added first TMS-$N_3$ (0.168 mL, 1.3 mmol) followed by *tert*-butyl nitrite (0.192 mL, 1.6 mmol) dropwise. The resulting mixture was allowed to reach rt. and stirred over-night. The volatiles were removed *in vacuo* and purification by preparative HPLC (20–80% B, over 20 min) afforded **19a** (0.12 g, 46%) as sticky oil. $^{1}$H NMR (600 MHz, DMSO-$d_6$): δ 12.57 (b s, 2H), 8.61 (t, $J$ = 5.8 Hz, 1H), 7.74 (d, $J$ = 8.0 Hz, 1H), 7.66 (s, 1H), 7.47 (dd, $J$ = 1.5, 8.0 Hz, 1H), 7.42 (d, $J$ = 1.5 Hz, 1H), 4.02 (b d, $J$ = 7.9 Hz, 2H), 3.95 (d, $J$ = 5.8 Hz, 2H), 2.89 (tt, $J$ = 3.2, 11.7 Hz, 1H), 2.79 (b s, 2H), 1.81 (b d, $J$ = 13.0 Hz, 2H), 1.43 (dq, $J$ = 3.7, 12.5 Hz, 2H), 1.40 (s, 9H). $^{13}$C NMR (600 MHz, DMSO-$d_6$): δ 171.0, 164.9, 153.8, 138.2, 137.3, 137.1, 130.8, 124.8, 123.3, 122.1, 122.0, 117.6, 78.6, 43.8, 41.3, 33.2, 31.9, 28.1. HRMS (ESI-TOF): *m/z* calculated for $C_{22}H_{28}N_7O_6$ $[M + H]^+$, 486.2096. Found, 486.2081 (ΔM = 3.0 ppm).

**(2-Azido-4-(4-(1-(*tert*-butoxycarbonyl)piperidin-4-yl)-1-hydroxy-1*H*-pyrazol-5-yl)benzoyl)glycine (19b).** In an amberized flask and under an argon atmosphere, a suspension of **18b** (0.45 g, 1.0 mmol) in anhydrous acetonitrile (40 mL) and THF (40 mL) was cooled to 0 °C and added first TMS-$N_3$ (0.312 mL, 2.4 mmol) followed by *tert*-butyl nitrite (0.35 mL, 2.9 mmol) dropwise. The resulting mixture was allowed to reach rt. and stirred over-night. The volatiles were removed *in vacuo* and purification by preparative HPLC (40–80% B, over 25 min) afforded **19b** (0.30 g, 62%) as sticky oil. $^1$H NMR (MeOD-*d*$_4$, 600 MHz): δ 7.94 (d, *J* = 8.0 Hz, 1H), 7.43 (d, *J* = 1.4 Hz, 1H), 7.39 (dd, *J* = 1.4, 8.0 Hz, 1H), 7.22 (s, 1H), 4.14 (s, 2H), 4.14–4.09 (m, 2H), 2.90–2.70 (m, 3H), 1.83–1.75 (m, 2H), 1.55 (qd, *J* = 4.0, 12.7 Hz, 2H), 1.45 (s, 9H). $^{13}$C NMR (MeOD-*d*$_4$, 150 MHz): δ 172.9, 167.8, 156.5, 139.5, 134.3, 132.2, 132.1, 130.5, 127.0, 126.9, 123.9, 121.2, 81.0, 45.7, 44.9, 42.5, 34.6, 43.4, 33.7, 28.7. HRMS (ESI-TOF): *m/z* calculated for $C_{22}H_{28}N_7O_6$ $[M + H]^+$, 486.2096. Found, 486.2082 (ΔM = 2.7 ppm).

***tert*-Butyl 4-(3-(3-azido-4-((2,76-dioxo-80-(2-oxohexahydro-1*H*-thieno[3,4-*d*]imidazol-4-yl)-6,9,12,15,18,21,24,27,30,33,36,39,42,45,48,51,54,57,60,63,66,69,72-tricosaoxa-3,75-diazaoctacontyl)carbamoyl)phenyl)-1-hydroxy-1*H*-pyrazol-4-yl)piperidine-1-carboxylate (20a).** In an amberized vial and under an argon atmosphere, a solution of **19a** (67 mg, 0.15 mmol) in anhydrous DMF (1 mL) was added DIPEA (0.105 mL, 0.60 mmol). To this, a solution of PyBOP (83 mg, 0.16 mmol) in anhydrous DMF (1 mL) was added and the mixture was allowed to incubate for 60 seconds. Then, a solution of Biotin-$PEG_{23}$-$NH_2$ (185 mg, 0.14 mmol) in anhydrous DMF (2 mL) was added and the resulting reaction mixture was stirred over-night at rt. The crude reaction was evaporated *in vacuo* and purification of the resulting residue by preparative HPLC (40–52% B, over 6 minutes) afforded **20a** (80.9 mg, 33%) as oil. $^1$H NMR (MeOD-*d*$_4$, 600 MHz): δ 7.90 (d, *J* = 8.0 Hz, 1H), 7.52 (d, *J* = 1.3 Hz, 1H), 7.50 (dd, *J* = 8.0, 1.3

Hz, 1H), 7.48 (s, 1H), 4.49 (dd, *J* = 7.7, 4.8 Hz, 1H), 4.31 (dd, *J* = 7.9, 4.5 Hz, 1H), 4.14 (br d, *J* = 13.3 Hz, 2H), 4.10 (s, 2H), 3.64-3.61 (m, 88H), 3.59 (t, *J* = 5.4 Hz, 2H), 3.54 (t, *J* = 5.4 Hz, 2H), 3.45 (t, *J* = 5.4 Hz, 2H), 3.36 (t, *J* = 5.4 Hz, 2H), 3.20 (dt, *J* = 9.6, 4.8 Hz, 1H), 2.97 (tt, *J* = 11.9, 3.1 Hz, 1H), 2.93 (dd, *J* = 12.7, 5.0 Hz, 1H), 2.90-2.75 (br s, 2H), 2.71 (d, *J* = 12.7 Hz, 1H), 2.22 (t, *J* = 7.3 Hz, 2H), 1.90 (br d, *J* = 12.8 Hz, 2H), 1.74 (m, 1H), 1.67 (m, 2H), 1.61 (m, 1H), 1.17 (qd, *J* = 12.8, 4.2 Hz, 2H), 1.46 (s, 9H), 1.44 (m, 2H). HRMS (ESI-TOF): *m/z* calculated for $C_{80}H_{141}N_{11}O_{30}S$ $[M + 2H]^{2+}$, 883.9978. Found, 883.9988 (ΔM = 1.1 ppm).

***tert*-Butyl 4-(5-(3-azido-4-((2,76-dioxo-80-(2-oxohexahydro-1*H*-thieno[3,4-*d*]imidazol-4-yl)-6,9,12,15,18,21,24,27,30,33,36,39,42,45,48,51,54,57,60,63,66,69,72-tricosaoxa-3,75-diazaoctacontyl)carbamoyl)phenyl)-1-hydroxy-1*H*-pyrazol-4-yl)piperidine-1-carboxylate (20b).** In an amberized vial and under an argon atmosphere, a solution of **19b** (150 mg, 0.31 mmol) in anhydrous DMF (1 mL) was added DIPEA (0.216 mL, 1.24 mmol). To this, a solution of PyBOP (172 mg, 0.33 mmol) in anhydrous DMF (1 mL) was added and the mixture was allowed to incubate for 60 seconds. Then, a solution of Biotin-$PEG_{23}$-$NH_2$ (377 mg, 0.29 mmol) in anhydrous DMF (3 mL) was added and the resulting reaction mixture was stirred over-night at rt. The crude reaction was evaporated *in vacuo* and purification of the resulting residue by preparative HPLC (40–52% B, over 6 minutes) afforded **20b** (264 mg, 52%) as oil. $^1$H NMR (MeOD-$d_4$, 600 MHz): δ 7.94 (d, *J* = 8.0 Hz, 1H), 7.45 (d, *J* = 1.3 Hz, 1H), 7.40 (dd, *J* = 8.0, 1.3 Hz, 1H), 7.22 (s, 1H), 4.50 (dd, *J* = 7.8, 4.9 Hz, 1H), 4.31 (dd, *J* = 7.8, 4.5 Hz, 1H), 4.12 (m, 2H), 4.10 (s, 2H), 3.64-3.61 (m, 88H), 3.60 (t, *J* = 5.4 Hz, 2H), 3.54 (t, *J* = 5.4 Hz, 2H), 3.45 (t, *J* = 5.4 Hz, 2H), 3.36 (t, *J* = 5.4 Hz, 2H), 3.20 (dt, *J* = 9.6, 4.8 Hz, 1H), 2.92 (dd, *J* = 12.7, 5.0 Hz, 1H), 2.88-2.75 (br s, 2H), 2.76 (tt, *J* = 12.4, 3.5 Hz, 1H), 2.71 (d, *J* = 12.7 Hz, 1H), 2.22 (t, *J* = 7.3 Hz, 2H), 1.79 (br d, *J* = 13.3 Hz, 2H), 1.74 (m, 1H), 1.67 (m, 2H), 1.61 (m, 1H), 1.57 (m,

2H), 1.46 (s, 9H), 1.44 (m, 2H). HRMS (ESI-TOF): *m/z* calculated for $C_{80}H_{141}N_{11}O_{30}S$ [M + 2H]$^{2+}$, 883.9978. Found, 883.9765 (ΔM = 1.5 ppm).

**Muscimol binding assay**

Cortical synaptic membranes from male SPRD rats were prepared as previously described[38]. The membranes were stored at −18 °C until the day of the assay where they were washed five times with 50 mM Tris, HCl buffer (pH 7.4). The binding protocol was performed in 96-well microplates, as previously described[39]. In brief, compounds were incubated with radioligand and membranes on ice, filtered through GF/C filters (PerkinElmer) using a 96-well harvester (Packard), and rapidly washed three times with ice-cold buffer. After drying the filter plates, counts per minute (CPM) values were determined using liquid scintillation counting in a Packard TopCount microplate scintillator counter (PerkinElmer). CPM values were fitted by nonlinear regression using GraphPad Prism version 7.02 (GraphPad Software, La Jolla, CA, USA) and $IC_{50}$ values determined and converted to $K_i$ values using the Cheng-Prusoff equation[40].

**The FLIPR Membrane Potential Blue (FMP) assay**

The functional properties of the analogs were characterized at the human α1β2γ2S $GABA_A$Rs transiently expressed in tsA201 cells in the FMP assay essentially as previously described[28]. 2 × $10^6$ tsA201 cells were split into a 10 cm tissue culture plate and transfected the following day with 2 μg α1-pCDNA3.1, 2 μg β2-pCDNA3.1 and 4 μg γ2S-pCDNA3.1 using Polyfect as a DNA carrier according to the protocol by the manufacturer (Qiagen, West Sussex, UK). The day after the transfection cells were split into poly-D-lysine-coated black 96-well plates with clear bottom (BD Biosciences, Palo Alto, CA). 16-24 h later the medium was aspirated, and the cells were washed with 100 μL Krebs buffer [140 mM NaCl/4.7 mM KCl/2.5 mM $CaCl_2$/1.2 mM $MgCl_2$/11 mM HEPES/10 mM D-Glucose, pH 7.4]. 50 μL assay buffer was added to the wells (in the antagonist testing, various concentrations of the test compounds were dissolved in this buffer) and then an additional 50 μL assay buffer supplemented with 1.0 mg/ml FMP dye was added to each well. Then the plate was incubated at 37 °C in a humidified 5% $CO_2$ incubator for 30 min and assayed in a in a FLEXStation 3 BenchtopMulti-Mode Microplate Reader (Molecular Devices, Crawley, UK) measuring emission [in fluorescence units (FU)] at 565 nm caused by excitation at 525 nm before and up to 90 s after addition of 33.3 μL assay buffer supplemented with the test compound (testing for agonist activity) or GABA ($EC_{70}$-$EC_{90}$ in the assay, testing for antagonist activity). The experiments were performed in duplicate at least three times for each compound.

The data from the FMP assay were analyzed using KaleidaGraph3.08 (Synergy Software, Reading, PA). The concentration-inhibition curves for the compounds as antagonists were constructed based on the difference in the fluorescence units (△FU) between the maximal fluorescence recorded before and after application GABA. The data were fitted to sigmoidal curves

with variable slopes using nonlinear regression, and the $IC_{50}$ values were derived from these equations and fits.

**Cell culture and transient expression of $GABA_A$Rs in HEK293 cells**

HEK293 cells used for electrophysiology and imaging experiments were grown and maintained at 37 ºC in Dulbecco's modified Eagle's medium (DMEM) in a humidified incubator in 95% air / 5% $CO_2$. HEK cells grown to 70% confluency in a mono-layer on a 10 cm (diameter) culture dish, were lifted with 2 mL 0.05% trypsin-EDTA, quenched with 10 mL media, pelleted for 2 min at 1000xg, gently triturated in 1 mL fresh media, volume-density adjusted, and finally plated onto poly-L-lysine-coated coverslips and transfected using a calcium phosphate protocol. In short, murine α1, β2/3, and γ2 $GABA_A$R and enhanced green fluorescent protein (eGFP) pRK5 cDNAs, were mixed with 340 mM $CaCl_2$, and an equal volume of HEPES-buffered saline (HBS; 50 mM HEPES, 280 mM NaCl and 2.8 mM $Na_2HPO_4$, pH 7.2). 1 μg of each cDNA was used, and a total of 4 μg cDNA was used for each transfection. The cDNA-calcium phosphate suspension was applied to cells, which were incubated overnight, and used in experiments 18-48 h after transfection.

Note that β2 and β3 were used interchangeably in this study to assess for any differences in photo-labelling. The GABA binding site from α1β2γ2 and α1β3γ2 receptors are identical, and the ligand affinities and potencies are very similar between the isoforms used.

**Electrophysiology on HEK293 cells**

Whole-cell $GABA_A$R channel currents were recorded with an Axopatch 200B amplifier (Molecular Devices) where cells were voltage clamped at -60mV and routinely compensated for

series resistance (Rs) of at least 70%. Currents were low-pass Bessel filtered at 5 kHz (80 dB/decade), digitized at 50 kHz via a Digidata 1320A (Molecular Devices) and recorded to disk (Dell Optiplex 990). Patch pipettes with a resistance of 3-5 MΩ were filled with intracellular solution containing (mM): 120 CsCl, 1 $MgCl_2$, 11 EGTA, 33 TEA-OH, 10 HEPES, 1 $CaCl_2$, and 2 adenosine triphosphate; pH 7.10. Cells were continuously perfused with Krebs solution containing (mM): 140 NaCl, 4.7 KCl, 1.2 $MgCl_2$, 2.52 $CaCl_2$, 11 glucose and 5 HEPES; pH 7.4.

For the inhibitory concentration-response experiments on α1β2/3γ2 $GABA_A$Rs, the antagonist analogues were pre-applied for 5 seconds before co-application with 10 μM GABA (~EC65-85; see Mortensen et al.[41]) using a rapid Y-tube application system.

Analogues used in the study were initially dissolved in 100% v/v DMSO, and these stock solutions where then diluted at least 1000-fold to working concentrations in extracellular Krebs solution. This ensured that no artificial DMSO responses were observed in experiments.

The inhibitory whole-cell responses of the analogues were evaluated for their potency by constructing inhibition-concentration relationship curves and fitting the data using the following equation:

$$I/I_{max} = 1 - [1/1 + (IC_{50}/B)^n)],$$

where the $IC_{50}$ is the antagonist concentration (B) causing half-maximal inhibition of the GABA ($EC_{60\text{-}80}$) induced response. $IC_{50}$ values obtained from each individual experiment were converted to $pIC_{50}$ values (= –Log $IC_{50}$) which are distributed on a linear scale. Mean $pIC_{50}$ values ± standard error of the mean (SEM) of 4-12 experiments were subject to statistical analyses (ANOVA and Student's t-test). The potency histogram in Fig. 2B has two y-axes for mean $pIC_{50}$ values ± sem, and the $IC_{50}$ transform (note: error bars refer only to the $pIC_{50}$ scale/axis).

**Photo-inactivation experiments on HEK293 cells**

UV photoactivation was performed using an OBIS 375 nm laser (Coherent Inc., Santa Clara, USA) integrated into a photolysis rig based around a Nikon Eclipse FN1 microscope with custom-made light-path control (Cairn Research Ltd., Faversham, UK). UV light was delivered to the recorded cell via a 40xW NIR, 0.8 NA, water-immersion objective. The UV laser output was empirically adjusted to 2 mW (4% of operating power) during a 10 seconds preparation exposure, as an optimal balance between avoiding cell damage, but still maintaining plenty of power to induce photo-inactivation.

**Tracking GABA receptor mobility**

The mobilities of $\alpha1\beta2\gamma2$ $GABA_A$ receptors expressed in HEK293 cells were studied using quantum dots (QDs) photo-linked to the receptors via **3b**. Two main methods were attempted: Method 1 – Cells were washed with Krebs solution before being incubated for 2 min with 1 mM **3b**; the cell preparation was then UV exposed for 10 s before replacing the solution with 50 pM $QD_{655}$-streptavidin (Thermo Fisher Scientific) and left to incubate for another 2 min; cells were then washed before imaging; control cells were treated similarly but were not UV exposed. Method 2 – 0.5 mM **3b** was first incubated for 3 min with 25 pM $QD_{655}$-streptavidin; cells were washed and then incubated for 2 min with the **3b**-$QD_{655}$-streptavidin mix before UV exposure for 10 s (controls were not UV exposed); followed by washing cells in Krebs solution and imaging. A range of variations were attempted in terms of concentrations, incubation times, intensities of UV exposure, and number of washes. Nevertheless, specific binding was largely absent no matter the method and variation.

Due to this near absent specific binding with **3b**-$QD_{655}$, we re-assessed and verified our methodology using an engineered $GABA_A$ α1 subunit with an N-terminal α-bungarotoxin mimotope site ($\alpha1_{BBS}$) which was expressed with β2 and γ2 subunits. Cells were washed and incubated in 0.44 μM α-bungarotoxin-biotin (Thermo Fisher Scientific) for 2 min; cells were then washed before incubation with 50 pM $QD_{655}$-streptavidin for 1 min; cells were washed again before imaging/tracking of specifically-labelled $QD_{655}$-$\alpha1_{BBS}\beta2\gamma2$ $GABA_A$Rs. These re-valuation experiments were successful, thereby verifying our methodology.

**Molecular modelling and docking**

The 6HUK crystal structure of the human $\alpha1\beta3\gamma2$ $GABA_AR$[19] was used as the target for docking 4-PHP at the orthosteric site using the induced fit docking protocol and co-crystallized bicuculline as the centroid of the binding site, with default settings[42]. Subsequently **2d** was similarly docked also using the induced fit protocol as above, but with the highest scoring 4-PHP pose selected as a reference position with a 2.0 Å tolerance. A fully elongated PEG-biotin linker was then attached to the highest scoring **2d** pose obtained. The residue Arg120 (human; Arg119 for murine) of the α1 subunit, which caps the upper cavity of the binding site[43] and thus gates access to the extracellular environment, was changed to a rotamer which did not clash with the PEG linker. The ligand-bound receptor complex was subsequently minimized using MacroModel[44] with 5000 iterations using default settings. Binding site and cavity surfaces were visualized using the surface function of PyMol[45].

ASSOCIATED CONTENT

**Supporting Information**. The Supporting Information is available free of charge on the ACS Publications website at DOI: XXXX.

Correlation plot of ligand Ki, determined from ligand binding studies and IC50, deduced from electrophysiological analysis, labelling experiments and videos.

AUTHOR INFORMATION

**Corresponding Authors**

* Prof. Bente Frølund - Phone: +45 35336495; email: bfr@sund.ku.dk.

* Prof. Trevor G Smart - Phone: +44 (0)2076792013; email: t.smart@ucl.ac.uk.

**ORCIDs**

Bente Frølund: https://orcid.org/0000-0001-5476-6288

Trevor G. Smart: https://orcid.org/0000-0002-9089-5375

**Author Contributions**

J.K., B.M.B., and P.F. designed and synthesized the novel compounds, K.T.K. performed the MS and NMR analyses, T.E.S. performed the computer modelling, B.N. and A.A.J. performed the binding and FMP assay, respectively, M.M. designed and performed all electrophysiology, photolysis and QD experiments on HEK293 cells. The manuscript was mainly written by M.M., J.K., B.F., and T.G.S. with contributions from all other authors. All authors have given approval to the final version of the manuscript. ϕ M.M. and J.K. are as main project contributors considered joined co-authors of this paper.

**Funding Sources**

M.M. was funded by MRC UK and The Leverhulme Trust, J.K. and B.M.B. were funded by the Lundbeck Foundation, A.A.J. was supported by the Novo Nordisk Foundation, P.F. was funded by the L. Fredericq Foundation.

**Notes**

The authors declare no competing financial interest.

ABBREVIATIONS

FMP; FLIPR Membrane Potential Blue; $GABA_AR$, γ-aminobutyric acid type-A receptor; 4-PIOL, 5-(4-piperidyl)-3-hydroxyisoxazole; 4-PHP, 4-(4-piperidyl)-1-hydroxypyrazole; PEG, polyethylene glycol; QD, quantum dot; pdb, protein data bank.

**References**


1. Bhattacharjee, A.; Wallner, M.; Lindemeyer, A. K.; Olsen, R. W., $GABA_A$ Receptor Physiology and Pharmacology. Oxford University Press: 2018.
2. Vithlani, M.; Terunuma, M.; Moss, S. J., The dynamic modulation of $GABA_A$ receptor trafficking and its role in regulating the plasticity of inhibitory synapses. *Physiol. Rev.* **2011,** *91* (3), 1009-22.
3. Eckel, R.; Szulc, B.; Walker, M. C.; Kittler, J. T., Activation of calcineurin underlies altered trafficking of α2 subunit containing $GABA_A$ receptors during prolonged epileptiform activity. *Neuropharmacol.* **2015,** *88*, 82-90.
4. Jacob, T. C.; Moss, S. J.; Jurd, R., $GABA_A$ receptor trafficking and its role in the dynamic modulation of neuronal inhibition. *Nat. Rev. Neurosci.* **2008,** *9* (5), 331-43.
5. Sekine-Aizawa, Y.; Huganir, R. L., Imaging of receptor trafficking by using α-bungarotoxin-binding-site-tagged receptors. *Proc. Natl. Acad. Sci. U. S. A.* **2004,** *101* (49), 17114-17119.
6. Arttamangkul, S.; Quillinan, N.; Low, M. J.; Von Zastrow, M.; Pintar, J.; Williams, J. T., Differential Activation and Trafficking of μ-opioid Receptors in Brain Slices. *Mol. Pharmacol.* **2008,** *74* (4), 972-979.
7. Lorenz-Guertin, J. M.; Wilcox, M. R.; Zhang, M.; Larsen, M. B.; Pilli, J.; Schmidt, B. F.; Bruchez, M. P.; Johnson, J. W.; Waggoner, A. S.; Watkins, S. C.; Jacob, T. C., A versatile optical tool for studying synaptic $GABA_A$ receptor trafficking. *J. Cell. Sc.i* **2017,** *130* (22), 3933-3945.
8. Hannan, S.; Smart, T. G., Cell surface expression of homomeric $GABA_A$ receptors depends on single residues in subunit transmembrane domains. *J. Biol. Chem.* **2018,** *293* (35), 13427-13439.
9. Hayashi, T.; Yasueda, Y.; Tamura, T.; Takaoka, Y.; Hamachi, I., Analysis of Cell-Surface Receptor Dynamics through Covalent Labeling by Catalyst-Tethered Antibody. *J. Am. Chem. Soc.* **2015,** *137* (16), 5372-5380.
10. Cognet, L.; Groc, L.; Lounis, B.; Choquet, D., Multiple Routes for Glutamate Receptor Trafficking: Surface Diffusion and Membrane Traffic Cooperate to Bring Receptors to Synapses. *Sci. Signaling* **2006,** *2006* (327), pe13.
11. Mortensen, M.; Iqbal, F.; Pandurangan, A. P.; Hannan, S.; Huckvale, R.; Topf, M.; Baker, J. R.; Smart, T. G., Photo-antagonism of the $GABA_A$ receptor. *Nat. Commun.* **2014,** *5*, 4454.
12. Byberg, J. R.; Labouta, I. M.; Falch, E.; Hjeds, H.; Krogsgaard-Larsen, P.; Curtis, D. R.; Gynther, B. D., Synthesis and biological activity of a $GABA_A$ agonist which has no effect on benzodiazepine binding and of structurally related glycine antagonists. *Drug. Des. Deliv.* **1987,** *1* (4), 261-74.
13. Frølund, B.; Kristiansen, U.; Brehm, L.; Hansen, A. B.; Krogsgaard-Larsen, P.; Falch, E., Partial $GABA_A$ receptor agonists. Synthesis and in vitro pharmacology of a series of nonannulated analogs of 4,5,6,7-tetrahydroisoxazolo[5,4-c]pyridin-3-ol. *J. Med. Chem.* **1995,** *38* (17), 3287-96.
14. Møller, H. A.; Sander, T.; Kristensen, J. L.; Nielsen, B.; Krall, J.; Bergmann, M. L.; Christiansen, B.; Balle, T.; Jensen, A. A.; Frølund, B., Novel 4-(Piperidin-4-yl)-1-hydroxypyrazoles as γ-Aminobutyric $Acid_A$ Receptor Ligands: Synthesis, Pharmacology, and Structure-Activity Relationships. *J. Med. Chem.* **2010,** *53* (8), 3417-3421.
15. Geoghegan, K. F.; Johnson, D. S., Chemical proteomic technologies for drug target identification. *Annu. Rep. Med. Chem.* **2010,** (45), 354–360.

16. Bergmann, R.; Kongsbak, K.; Sørensen, P. L.; Sander, T.; Balle, T., A unified model of the $GABA_A$ receptor comprising agonist and benzodiazepine binding sites. *PLoS One* **2013,** *8* (1), e52323.
17. Sander, T.; Frølund, B.; Bruun, A. T.; Ivanov, I.; McCammon, J. A.; Balle, T., New insights into the $GABA_A$ receptor structure and orthosteric ligand binding: Receptor modeling guided by experimental data. *Proteins: Struct., Funct., Bioinf.* **2011,** *79* (5), 1458-1477.
18. Laverty, D.; Desai, R.; Uchanski, T.; Masiulis, S.; Stec, W. J.; Malinauskas, T.; Zivanov, J.; Pardon, E.; Steyaert, J.; Miller, K. W.; Aricescu, A. R., Cryo-EM structure of the human α1β3γ2 $GABA_A$ receptor in a lipid bilayer. *Nature* **2019,** *565* (7740), 516-520.
19. Masiulis, S.; Desai, R.; Uchanski, T.; Serna Martin, I.; Laverty, D.; Karia, D.; Malinauskas, T.; Zivanov, J.; Pardon, E.; Kotecha, A.; Steyaert, J.; Miller, K. W.; Aricescu, A. R., $GABA_A$ receptor signalling mechanisms revealed by structural pharmacology. *Nature* **2019,** *565* (7740), 454-459.
20. Zhu, S.; Noviello, C. M.; Teng, J.; Walsh, R. M., Jr.; Kim, J. J.; Hibbs, R. E., Structure of a human synaptic $GABA_A$ receptor. *Nature* **2018,** *559* (7712), 67-72.
21. Phulera, S.; Zhu, H.; Yu, J.; Claxton, D. P.; Yoder, N.; Yoshioka, C.; Gouaux, E., Cryo-EM structure of the benzodiazepine-sensitive α1β1γ2S tri-heteromeric $GABA_A$ receptor in complex with GABA. *Elife* **2018,** *7*.
22. Krall, J.; Jensen, C. H.; Sørensen, T. E.; Nielsen, B.; Jensen, A. A.; Sander, T.; Balle, T.; Frølund, B., Exploring the Orthosteric Binding Site of the γ-Aminobutyric Acid Type A Receptor using 4-(Piperidin-4-yl)-1-hydroxypyrazoles 3- or 5-Imidazolyl Substituted: Design, Synthesis, and Pharmacological Evaluation. *J. Med. Chem.* **2013,** *56* (16), 6536-6540.
23. Boddum, K.; Frølund, B.; Kristiansen, U., The $GABA_A$ antagonist DPP-4-PIOL selectively antagonises tonic over phasic GABAergic currents in dentate gyrus granule cells. *Neurochem. Res.* **2014,** *39* (11), 2078-84.
24. Krehan, D.; Storustovu, S. I.; Liljefors, T.; Ebert, B.; Nielsen, B.; Krogsgaard-Larsen, P.; Frølund, B., Potent 4-arylalkyl-substituted 3-isothiazolol $GABA_A$ competitive/noncompetitive antagonists: synthesis and pharmacology. *J. Med. Chem.* **2006,** *49* (4), 1388-96.
25. Albertoni, B.; Hannam, J. S.; Ackermann, D.; Schmitz, A.; Famulok, M., A trifluoromethylphenyl diazirine-based SecinH3 photoaffinity probe. *Chem. Commun. (Cambridge, U. K.)* **2012,** *48* (9), 1272-4.
26. Sakurai, K.; Ozawa, S.; Yamada, R.; Yasui, T.; Mizuno, S., Comparison of the reactivity of carbohydrate photoaffinity probes with different photoreactive groups. *ChemBioChem* **2014,** *15* (10), 1399-403.
27. Smith, E.; Collins, I., Photoaffinity labeling in target- and binding-site identification. *Future Med. Chem.* **2015,** *7* (2), 159-83.
28. Weber, P. J.; Beck-Sickinger, A. G., Comparison of the photochemical behavior of four different photoactivatable probes. *J. Pept. Res.* **1997,** *49* (5), 375-83.
29. Frølund, B.; Jensen, L. S.; Guandalini, L.; Canillo, C.; Vestergaard, H. T.; Kristiansen, U.; Nielsen, B.; Stensbøl, T. B.; Madsen, C.; Krogsgaard-Larsen, P.; Liljefors, T., Potent 4-aryl- or 4-arylalkyl-substituted 3-isoxazolol $GABA_A$ antagonists: synthesis, pharmacology, and molecular modeling. *J. Med. Chem.* **2005,** *48* (2), 427-39.
30. Frølund, B.; Jørgensen, A. T.; Tagmose, L.; Stensbol, T. B.; Vestergaard, H. T.; Engblom, C.; Kristiansen, U.; Sanchez, C.; Krogsgaard-Larsen, P.; Liljefors, T., Novel class of potent 4-arylalkyl substituted 3-isoxazolol $GABA_A$ antagonists: synthesis, pharmacology, and molecular modeling. *J. Med. Chem.* **2002,** *45* (12), 2454-68.

31. Frølund, B.; Jensen, L. S.; Storustovu, S. I.; Stensbøl, T. B.; Ebert, B.; Kehler, J.; Krogsgaard-Larsen, P.; Liljefors, T., 4-aryl-5-(4-piperidyl)-3-isoxazolol $GABA_A$ antagonists: synthesis, pharmacology, and structure-activity relationships. *J. Med. Chem.* **2007,** *50* (8), 1988-92.
32. Miziak, P.; Zon, J.; Amrhein, N.; Gancarz, R., Inhibitors of phenylalanine ammonia-lyase: substituted derivatives of 2-aminoindane-2-phosphonic acid and 1-aminobenzylphosphonic acid. *Phytochem.* **2007,** *68* (4), 407-15.
33. Suhana, H.; Srinivasan, P. C., A Facile Synthesis of 1,4-Diacylbenzenes. *Synth. Commun.* **2003,** *33* (18), 3097–3102.
34. Hannan, S.; Wilkins, M. E.; Thomas, P.; Smart, T. G., Tracking cell surface mobility of GPCRs using α-bungarotoxin-linked fluorophores. *Methods Enzymol.* **2013,** *521*, 109-29.
35. Generalov, R.; Kavaliauskiene, S.; Westrom, S.; Chen, W.; Kristensen, S.; Juzenas, P., Entrapment in phospholipid vesicles quenches photoactivity of quantum dots. *Int. J. Nanomed.* **2011,** *6*, 1875-88.
36. Felding, J.; Kristensen, J.; Bjerregaard, T.; Sander, L.; Vedsø, P.; Begtrup, M., Synthesis of 4-Substituted 1-(Benzyloxy)pyrazoles via Iodine−Magnesium Exchange of 1-(Benzyloxy)-4-iodopyrazole. *J. Org. Chem.* **1999,** *64* (11), 4196-4198.
37. Gottlieb, H. E.; Kotlyar, V.; Nudelman, A., NMR Chemical Shifts of Common Laboratory Solvents as Trace Impurities. *J. Org. Chem.* **1997,** *62* (21), 7512-7515.
38. Ransom, R. W.; Stec, N. L., Cooperative modulation of [3H]MK-801 binding to the N-methyl-D-aspartate receptor-ion channel complex by L-glutamate, glycine, and polyamines. *J Neurochem.* **1988,** *51* (3), 830-6.
39. Giraudo, A.; Krall, J.; Nielsen, B.; Sørensen, T. E.; Kongstad, K. T.; Rolando, B.; Boschi, D.; Frølund, B.; Lolli, M. L., 4-Hydroxy-1,2,3-triazole moiety as bioisostere of the carboxylic acid function: a novel scaffold to probe the orthosteric gamma-aminobutyric acid receptor binding site. *Eur. J. Med. Chem.* **2018,** *158*, 311-321.
40. Leff, P.; Dougall, I. G., Further concerns over Cheng-Prusoff analysis. *Trends Pharmacol. Sci* **1993,** *14* (4), 110-2.
41. Mortensen, M.; Patel, B.; Smart, T. G., GABA Potency at $GABA_A$ Receptors Found in Synaptic and Extrasynaptic Zones. *Front. Cell Neurosc.i* **2011,** *6*, 1.
42. 2019-2, S. R. *Schrödinger Suite 2019-2 Induced Fit Docking protocol; Glide, Schrödinger, LLC, New York, NY, 2019; Prime, Schrödinger, LLC, New York, NY, 2019.*
43. Krall, J.; Balle, T.; Krogsgaard-Larsen, N.; Sørensen, T. E.; Krogsgaard-Larsen, P.; Kristiansen, U.; Frølund, B., $GABA_A$ receptor partial agonists and antagonists: structure, binding mode, and pharmacology. *Adv. Pharmacol.* **2015,** *72*, 201-27.
44. 2019-2, S. R. *MacroModel, Schrödinger, LLC, New York, NY, 2019.*, version 9.8; 2019.
45. PyMOL *The PyMOL Molecular Graphics System, Version 2.2.0 Schrödinger, LLC.*

**TOC**

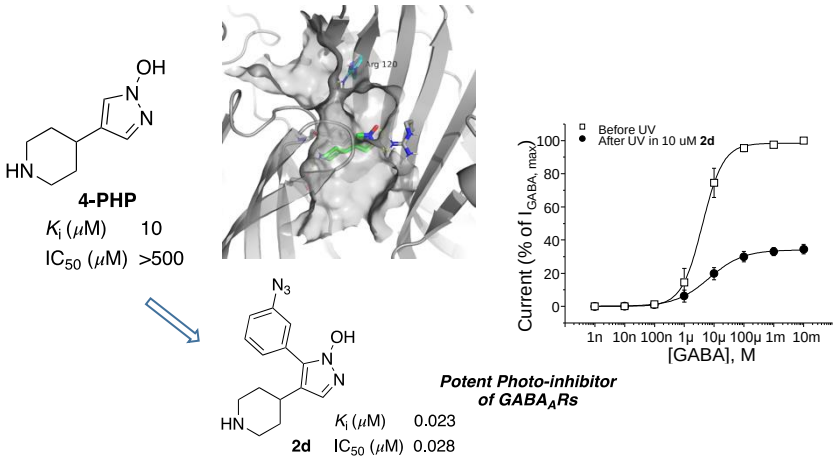
OH
N
N
HN
4-PHP
$K_i$ ($\mu$M) 10
$IC_{50}$ ($\mu$M) >500
Arg 120
$N_3$
OH
N
N
HN
2d
$K_i$ ($\mu$M) 0.023
$IC_{50}$ ($\mu$M) 0.028
Before UV
After UV in 10 uM 2d
Current (% of $I_{GABA, max}$)
100
80
60
40
20
0
1n 10n 100n 1µ 10µ 100µ 1m 10m
[GABA], M
*Potent Photo-inhibitor of $GABA_A$Rs*